AD-A082 750 NATIONAL AVIATION FACILITIES EXPERIMENTAL CENTER ATL--ETC F/G 17/9
DESIGN OF AN IMPROVED WEATHER CONTOURING DEVICE.(U)
MAR 80 R G OLIVER

UNCLASSIFIED FAA-NA-79-39 FAA-RD-80-6 NL

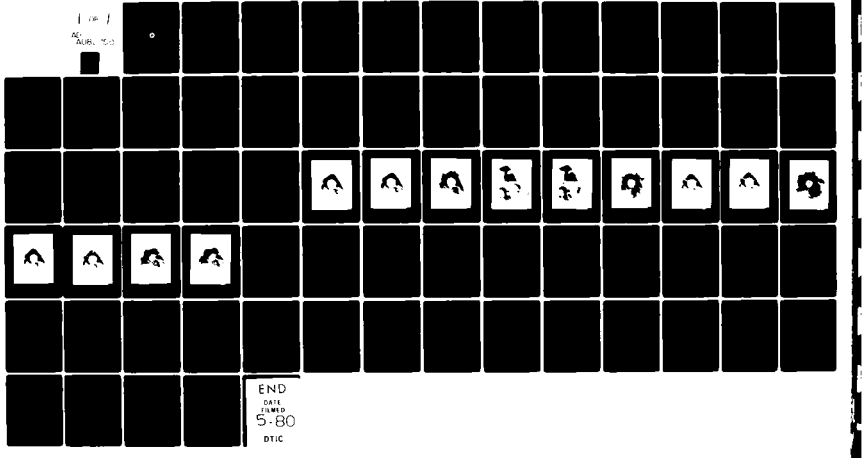

END
DATE FILMED
5-80
DTIC

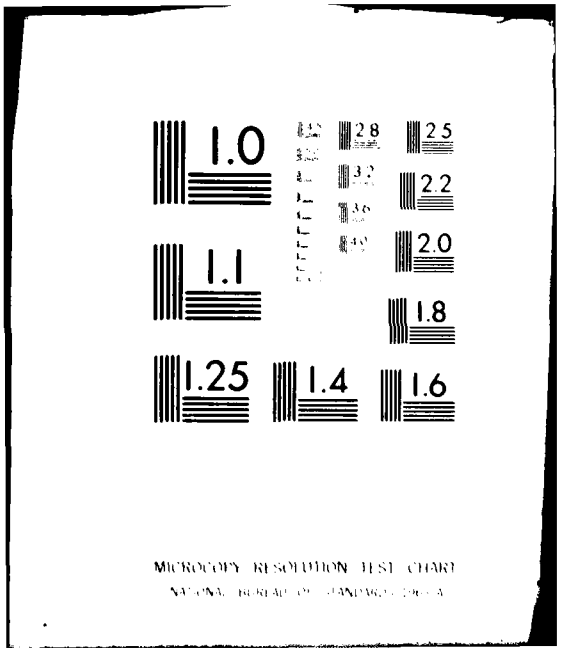
1.0
1.1
1.25
1.4
1.6
1.8
2.0
2.2
2.5
2.8
3.2
3.6
4.0
MICROCOPY RESOLUTION TEST CHART

Report No. FAA-RD-80-6

DESIGN OF AN IMPROVED WEATHER CONTOURING DEVICE

Robert G. Oliver

MARCH 1980

FINAL REPORT

Prepared for

U.S. DEPARTMENT OF TRANSPORTATION
FEDERAL AVIATION ADMINISTRATION
Systems Research & Development Service
Washington, D.C. 20590

NOTICE

The United States Government does not endorse products or manufacturers. Trade or manufacturer's names appear herein solely because they are considered essential to the object of this report.

Technical Report Documentation Page

1. Report No.	2. Government Accession No.	3. Recipient's Catalog No.
FAA-RD-80-6		

4. Title and Subtitle

DESIGN OF AN IMPROVED WEATHER CONTOURING DEVICE,

5. Report Date	
	March 1980
6. Performing Organization Code	
8. Performing Organization Report No.	FAA-NA-79-39

7. Author(s)

Robert G. Oliver

9. Performing Organization Name and Address

Federal Aviation Administration
National Aviation Facilities Experimental Center
Atlantic City, New Jersey 08405

10. Work Unit No. (TRAIS)	
11. Contract or Grant No.	021-241-820
13. Type of Report and Period Covered	Final rept. Nov 77-Sep 78
14. Sponsoring Agency Code	

12. Sponsoring Agency Name and Address

U.S. Department of Transportation
Federal Aviation Administration
Systems Research and Development Service
Washington, D.C. 20590

15. Supplementary Notes

16. Abstract

A prototype weather contouring device was developed and built by the National Aviation Facilities Experimental Center (NAFEC) to aid in the preparation of procurement specifications. The device uses the new concept of contour symbol generation to produce lines, shaded areas, or other symbols necessary to generate contours of weather intensity. Unlike former techniques, this device generates homogenous lines and is easily programmable for other formats. The device can provide dots or other symbols to the more intense side of a weather contour line clearly aiding the interpretation of the weather display.

The device is designed to take advantage of digital signal transmission techniques for the transmission of up to six levels of weather intensity. Any two of these six levels can be simultaneously displayed. The device was designed for those applications where plan position indicator (rho-theta) format is desired or necessary. Tests indicate that the device can generate contours which are exceptionally smooth and stable and are well suited to use in the air traffic control system.

17. Key Words	18. Distribution Statement
Weather Contouring Air Traffic Control Display Digital Weather Processing Radar	Document is available to the U. S. public through the National Technical Information Service, Springfield, Virginia 22161

19. Security Classif. (of this report)	20. Security Classif. (of this page)	21. No. of Pages	22. Price
Unclassified	Unclassified	70	

Form DOT F 1700.7 (8-72) Reproduction of completed page authorized

METRIC CONVERSION FACTORS

Approximate Conversions to Metric Measures

Symbol	When You Know	Multiply by	To Find	Symbol
		LENGTH		
in	inches	*2.5	centimeters	cm
ft	feet	30	centimeters	cm
yd	yards	0.9	meters	m
mi	miles	1.6	kilometers	km
		AREA		
in^2	square inches	6.5	square centimeters	cm^2
ft^2	square feet	0.09	square meters	m^2
yd^2	square yards	0.8	square meters	m^2
mi^2	square miles	2.6	square kilometers	km^2
	acres	0.4	hectares	ha
		MASS (weight)		
oz	ounces	28	grams	g
lb	pounds	0.45	kilograms	kg
	short tons (2000 lb)	0.9	tonnes	t
		VOLUME		
tsp	teaspoons	5	milliliters	ml
Tbsp	tablespoons	15	milliliters	ml
fl oz	fluid ounces	30	milliliters	ml
c	cups	0.24	liters	l
pt	pints	0.47	liters	l
qt	quarts	0.96	liters	l
gal	gallons	3.8	liters	l
ft^3	cubic feet	0.03	cubic meters	m^3
yd^3	cubic yards	0.76	cubic meters	m^3
		TEMPERATURE (exact)		
°F	Fahrenheit temperature	5/9 (after subtracting 32)	Celsius temperature	°C

*1 in = 2.54 (exactly). For other exact conversions and more detailed tables, see NBS Misc. Publ. 286, Units of Weights and Measures, Price $2.25, SD Catalog No. C13.10:286.

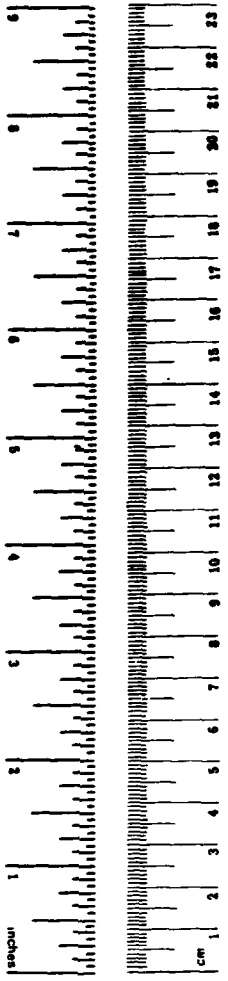

Approximate Conversions from Metric Measures

Symbol	When You Know	Multiply by	To Find	Symbol
		LENGTH		
mm	millimeters	0.04	inches	in
cm	centimeters	0.4	inches	in
m	meters	3.3	feet	ft
m	meters	1.1	yards	yd
km	kilometers	0.6	miles	mi
		AREA		
cm^2	square centimeters	0.16	square inches	in^2
m^2	square meters	1.2	square yards	yd^2
km^2	square kilometers	0.4	square miles	mi^2
ha	hectares (10,000 m^2)	2.5	acres	
		MASS (weight)		
g	grams	0.035	ounces	oz
kg	kilograms	2.2	pounds	lb
t	tonnes (1000 kg)	1.1	short tons	
		VOLUME		
ml	milliliters	0.03	fluid ounces	fl oz
l	liters	2.1	pints	pt
l	liters	1.06	quarts	qt
l	liters	0.26	gallons	gal
m^3	cubic meters	35	cubic feet	ft^3
m^3	cubic meters	1.3	cubic yards	yd^3
		TEMPERATURE (exact)		
°C	Celsius temperature	9/5 (then add 32)	Fahrenheit temperature	°F

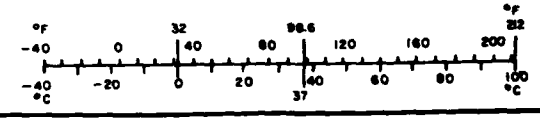

PREFACE

Acknowledgment is made to the following people for their contribution to this project: Mr. Edwin Hartz, National Aviation Facilities Experimental Center (NAFEC), for his help in constructing the hardware used in this project and in coordinating with the people at Terminal Automation Test Facility (TATF) at NAFEC to set up the equipment demonstrations; and Mr. John Wiley, Co-Op, Drexel University, NAFEC, for the construction of the support and test hardware for this project and for meticulously coding the decision algorithm for the contour generator.

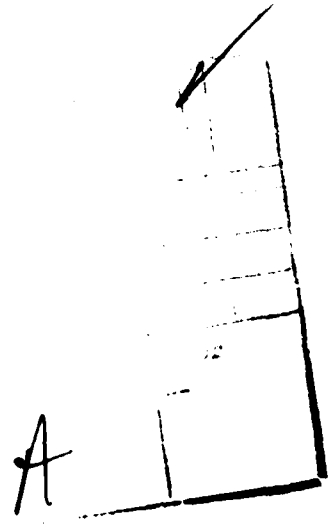

TABLE OF CONTENTS

LIST OF ILLUSTRATIONS

LIST OF ILLUSTRATIONS (Continued)

INTRODUCTION

PURPOSE.

The purpose of this project was to develop and build a prototype weather contouring device to aid in the preparation of a procurement specification. The device was to be retrofitted to the Airport Surveillance Radar (ASR-8) and be usable on any conventional plan position indicator (PPI). It was to provide two specific contour types chosen by the Air Traffic Service personnel. Each type is capable of displaying two of a possible six predetermined levels of weather intensity.

The contours produced by this device were to be related to units of reflectivity (dBZ) rather than simply received power or some equally arbitrary units. It was assumed that the input video would be log normal, and no attempt was made to solve the moving target indicator (MTI) velocity response or MTI limiting problems, even though MTI must be used in a practical system.

BACKGROUND.

The advent of circular polarization (CP), logarithmic fast time constant (LOG FTC), and other techniques for eliminating weather from the air traffic controllers' display has made it desirable to provide weather information to the operator in other than the original raw radar form, specifically to provide the air traffic controller with continuous weather information superimposed on the air traffic control (ATC) display in a form that does not interfere with the detection and control of aircraft targets. This display of weather on the controller display has generally been called weather contouring.

Weather contouring originally referred to the generation of a thin isoreflectivity line along the weather system perimeter. Later, the term was expanded to include any processed display of weather reflectivity. Weather contours were lines generated by displaying values of reflectivity between Z and $Z + \Delta Z$, where Z was the threshold level and ΔZ was an arbitrarily small reflectivity increment. For small ΔZ and a smooth weather function, this produced a smooth, continuous isoreflectivity line. In reality, weather returns do not produce a well-defined, smooth function and so do not produce smooth or continuous contours. An increase in the value of ΔZ coupled with range smoothing of the weather video signal causes the generated lines to be continous and also somewhat wide and therefore tends to mask out the discontinuities of the contour. This is not without cost, since weather near the threshold which does not change abruptly will produce excessively wide lines adversely affecting resolution and cluttering the display.

Elimination of the varying line width could be accomplished with the introduction of a single-pulse generating circuit (one-shot) after the threshold operation. This generates lines with constant radial dimension. However, many of the lines which are needed to outline weather are in the radial direction and require radial dimensions much larger than the single-pulse width. The single-pulse circuit produces discontinuities in this instance.

Also, the early weather contouring systems produced misregistration in range and azimuth caused by the time delay introduced by the contouring process.

In response to a request by the Federal Aviation Administration (FAA), Air Traffic Service (ATS) for improved weather detection and display capabilities for the ATC radar system, the device described in this report was developed by the National Aviation Facilities Experimental Center (NAFEC) to meet the need for improved display of weather information and to solve the above problems.

DESCRIPTION OF EQUIPMENT REQUIREMENT

DISCUSSION.

A weather cell is composed of a large number of small targets; i.e., raindrops, which move slightly between radar samples. When the raindrops are positioned such that the returned signals add together mostly in phase with one another, the received signal is large. When the returned signals add together mostly out of phase, the received signal is small. It is this variation of the received signal that causes the principal weather display problem. Note that any given measurment of the amplitude of a weather cell can vary from the mean by a considerable amount; in fact, variations of greater than 5 decibels (dB) can be expected about half of the time.

To make a better estimate of the weather amplitude, several samples must be averaged together. The greater the number of samples averaged, the better the estimate. This averaging can be accomplished in three ways: (1) averaging consecutive pulses in range, (2) averaging adjacent range segments in azimuth, and (3) averaging over a given area for a number of consecutive antenna scans. Range and scan averaging increase the number of effective independent samples by the actual number of samples averaged, while, because of the signal correlation in azimuth, azimuth averaging increases the number of effective samples by a factor less than the number of actual averaged samples. Both range and azimuth averaging reduce the spatial resolution of the weather display. Typically, the accuracy of the weather display is determined by the required resolution and the resolution inherent in the radar system itself. These topics are discussed in the following sections.

It must be noted that the requirement to produce weather contours in terms of reflectivity rather than power or other units was actually of minor importance in this effort. This is not to say that the requirement is not important, but rather that the weather contour device to be built would be inherently accurate and so not affect the calibration.

The calibration of the weather detection system is overwhelmingly influenced by the characteristics of the radar with which it is employed. Effects of sensitivity time control (STC), circular polarization (CP), and the MTI can introduce errors considerably greater in magnitude than can be expected by implementing any averaging or thresholding techniques.

WEATHER DISPLAY ACCURACY.

One of the measures of system performance is the accuracy with which the weather cell can be displayed. This accuracy can be measured in two related ways called level accuracy and positional accuracy. Level accuracy is a measure of the variation in the actual weather reflectivity that causes a contour to be generated in a given cell. Positional accuracy is a measure of the variation in the generated contour from the actual position of the threshold crossing of the weather. The level accuracy is dependent on the averaging done before the threshold decision. It is not a function of the weather geometry.

The level accuracy is computed by considering the effects of averaging on log normal video. The standard deviation of the weather reflectivity is 5.57 dB. After averaging, the standard deviation is reduced to 0.36 dB. This is equivalent to averaging over 80 independent samples, 16 of which are derived from the range averaging and 5 of which are derived from azimuth averaging (calculated in appendix A). The resolution cell size necessary to generate this number of independent samples is 0.8 nautical miles (nmi) by 1.4°.

The positional accuracy of the system is roughly equivalent to the display accuracy. Unlike level accuracy, the positional accuracy of the system is a function of the storm characteristics; namely, the gradient of the reflectivity (change of reflectivity with distance). If the storm has a high gradient, the edges are fairly well defined, and no problem results. If the gradient is low, considerable error can be introduced by small variations in weather level. The effect of a small change in level gradient on the presentation of a weather cell with high and low reflectivity is shown in figure 1.

As more samples are taken, the positional accuracy decreases. This effect is particularly pronounced when the azimuth time constant is increased, because the signals take a long time to decay and tend to elongate the contours in the azimuth direction. This is a common side effect of integration. On observing the display, the averaging parameters which seemed to produce the best display were 0.8 nmi of range averaging, and five independent samples in azimuth.

DISPLAY RESOLUTION.

The resolution limits of the display depend on the operational requirements of the air traffic controller. It is difficult to quantify this requirement, since it depends not only on the weather characteristics, but also on the characteristics of the display and the preferences of the controller using the display.

The display resolution was chosen to produce a nearly square cell 0.4 nmi on a side at 16 nmi. This corresponds to an azimuth dimension of about 1.4°, which is just slightly larger than an antenna beam width, which is the minimum resolution attainable in azimuth. Weather displays for radar typically use dimensions of this order.

The display cell size was somewhat smaller than the actual resolution of the system. This was because it was felt that the coarseness of the presentation using the actual system resolution would seriously detract from the appearance of the display. In fact, without the deholing and character generation (to be discussed later), the display would probably be unusable even with a resolution this large.

WEATHER CONTOURING.

The display of discrete weather information on a radar display is referred to as contouring. One way to display these data is by thin isoreflectivity lines in much the same way as altitude is displayed on a topographic map. This has the advantage of disturbing very little of the display (at least in theory) and contributing very little of the total display brightness. In past systems, the raggedness of the contours has been the primary objection to their use. This raggedness is caused by the inherent fluctuation of the storm cell as was discussed above in BACKGROUND. This has largely been overcome in the NAFEC system by improved averaging and processing techniques. Another way to display weather is by shading the interior of the contour lines. This creates a display in which the reflectivity of the weather cell is indicated by the brightness of the shading. This system uses two levels of such shading to indicate the presence of weather above two preset thresholds. Typically, these thresholds would be chosen to indicate moderate and severe weather. Combinations of these two techniques are also possible as in the second proposal below.

ATS personnel in cooperation with FAA Systems Research and Development Service (SRDS) proposed the following two contours for implementation in this device. The first contour type (called contour type 1) is the shaded version described above; i.e., two threshold levels indicated by two levels of intensity shading. The second type (called contour type 2) consists of a low-level intensity shading to indicate the upper threshold level and a continuous isoreflectivity line to indicate the lower threshold level. An illustration of these proposals is shown in the first two figures of figure 2.

There are several advantages of the first proposal. For example, there is no ambiguity in deciding if any given area contains weather, especially when the contour line extends off the visible area of the PPI, causing uncertainty as to which side of the contour contains weather and which does not. The shaded version is simple to produce, and it ordinarily would not require as much smoothing as the line contour, because the eye tends to integrate jagged contours of this type better than thin-line contours.

The advantage of the second proposal is primarily the absence of a weather presentation over much of the display area. It was hoped that this would minimize the interference between the ATC presentation and the weather presentation.

A third idea (contour type 3) which was also implemented was the addition of a series of dots on the weather side of the proposed line contour. This technique removes the ambiguity when the entire contour line was not visible.

SYMBOLIC REPRESENTATION.

To efficiently develop a system to generate a variety of contours, it was first necessary to find a method for displaying the required information as a set of smaller, easy-to-generate elements. The approach used is similar to that used to generate characters on a cathode-ray tube (CRT) for alphanumeric displays. Each range azimuth cell is decomposed into an eight-by-eight array of smaller dots. This enables the device to generate one of a set of specialized symbols chosen for contour representation. The symbols are shown in appendix B pages B-1 to B-9. This technique results in the improved quality of the weather presentation. To use this technique, the contour device must possess some algorithm to determine which contour element to generate at any given time. This is not a trivial problem, and no attempt was made to solve this problem analytically. Instead, the "algorithm," consisting mainly of judgment and intuition, was accomplished by hand for every possible case and then coded into a read-only memory (ROM) for the hardware implementation. This list is shown in appendix B pages B-10 to B-22. The principal advantages of this system are the almost complete flexibility of the contours possible and the ease with which they are implemented. Only 64 eight-bit words must be coded to change the contour type, and none of these affect the decision coding.

DESCRIPTION OF EQUIPMENT.

The contour generator is built in a 19- by 10-inch rack-mounted cabinet and contains all of the hardware for contour generation. This would normally be separated into two sections, one at the radar site and the other at the indicator site. The system can accept triggers, video, and azimuth information from one source and simultaneously generate video synchronized to the triggers and azimuth information from another, possibly different, source. The constants of integration and range averaging are adjustable from the front panel. Also, the contour level, type, and the deholer function are front-panel controllable.

THEORY OF OPERATION AND SYSTEM TESTS

This section describes the functional operation of the contouring device. The signal flow can be traced on the system block diagram shown in figure 3. In addition, a simplified schematic diagram is presented for each subunit in figures 4 through 9. Timing diagrams and other discriptive diagrams are shown in figures 10 through 15. Attention is given to the processing performed by each unit of the contouring device, and no attempt is made to provide a complete technical description of the type usually found in instruction manuals.

RANGE AVERAGING.

The range averaging process is accomplished in two steps. The first is integration over a 2.4-microsecond interval using an analog integrator, and the second is the digital summation of from one to four analog samples. The incoming signal is first converted into a current in the voltage-to-current converter (see figure 4). The current derived in the converter is used to charge one of two capacitors, C1 or C2. These capacitors are charged alternately and sampled by the analog-to-digital (A/D) converter when they are not being charged. The timing for this operation is illustrated in figure 10. Notice that the capacitor voltage is stable during the A/D conversion, so a sample-and-hold circuit is not necessary. The capacitor voltage at the end of the interval is given by $\frac{1}{C}\int_0^t I(t)dt$, and since the current, I(t), is given by $I(t)=gV(t)$, where g is the transconductance of the voltage-to-current converter, the final capacitor voltage is seen to be $V_c=\frac{g}{C}\int_0^t V(t)dt$, the integral of the input voltage with respect to time.

The problem with this technique is that the capacitors are temperature sensitive. This effectively changes the gain of the integrator and causes fluctuation of the generated contours. Since this only affected the absolute calibration of the signal and not the quality of the display, these changes were tolerated. This problem could be corrected by using an improved method of analog integration or faster conversion and exclusively digital averaging.

The digital summation is accomplished by delaying and inverting the input signal and then summing this signal with the input in a recursive adder (see figure 4). The response of this circuit is seen to be a running sum of the previous n pulses, where n is determined by the delay time introduced prior to summation. This delay is varied by changing the clock rate of the delay shift register to change the summation from one through four samples integrated. The timing for this operation is shown in figure 11. A photograph of the processed signal after range averaging is shown in figure 16.

As can be seen from this photograph, the range averaging produces a smoothing effect only in the radial direction. This can be observed as a range elongation of virtually all targets. Notice that there seems to be very little azimuth correlation. This is still not suitable for thresholding.

AZIMUTH AVERAGING.

Averaging in azimuth was accomplished after range averaging by a conventional digital integrator. The schematic diagram of this device is shown in figure 5. The integration cell size is 4.8 microseconds, and there are 160 such cells in range. For each of these cells, the video input is compared to the current contents of the cell. This represented the exponentially weighted average of the past cells. A fraction of the difference was added to the cell contents. The multiplier of the difference determined the time constant of the integrator.

The multiplier could be one of four values, 1/8, 1/16, 1/32, and 1/64. This corresponds to the sampling of from 15 to 127 effective samples as described in appendix C. The last two time constants are for test purposes only and are not useful in operation, since they correspond to averaging over four to eight beamwidths. The combined effect of averaging in range and azimuth produces the two-dimensional weighting function shown in figure 12.

A photograph of the system output after azimuth filtering is shown in figure 17. Notice that the picture seems to be blurred due to the low-pass filtering. This is evidence of data smoothing in the azimuth direction. This is much more suitable for thresholding than the range-averaged-only signal. The transfer function of this filter is discussed in detail in appendix C prior to the calculation of effective samples.

THRESHOLDING.

Thresholding occurred at six independently set levels. These levels were selectable to about 1 dB on a 60-dB dynamic range log scale. Each level had a hysteresis of about 1 dB in an attempt to reduce the noise contribution for storms with very low gradients. If the input signal is greater than 0.5 dB above the threshold, a threshold crossing is declared by setting the associated threshold flip-flop. To reset the threshold flip-flop, the signal must drop to a level below -0.5 dB of the threshold level. This is the digital equivalent of the Schmitt trigger, commonly used for the detection of digital signals in the presence of noise. Referring to figure 6, the comparators set the flip-flop when the signal input was greater than the threshold setting. The comparators reset the flip-flop when the signal was less than the threshold setting. When the signal was equal to the threshold setting, no change occurred. The threshold and input were both quantized to five bits. It is this quantization that sets the threshold hysteresis. The transfer function for this circuit with a typical input is shown in figure 13. After the threshold decision was made, the flip-flop outputs were encoded to produce a three-bit binary number representing the highest threshold crossed. It was this number that was processed in the remaining sections of the system. A photograph of the threshold output is shown in figure 18. The intensity indicates the threshold level. Notice that the edge of the thresholded signal is reasonably smooth and continuous. This would not be the case without prior range and azimuth smoothing.

SCAN STORAGE (WEATHER MAP).

After the signal is thresholded, it is stored in a memory organized as a 160-by-256-cell range-azimuth map. This storage was necessary for realignment of the averaged weather to superimpose the contour over the location of the weather. In practice, the weather contours appear slightly less than one antenna scan late. This was not a problem, because of the slow moving nature of weather. In the case where some form of slow-speed data transmission is used, the data would show up some minutes late, regardless of this effect. This also provides an easy method of aligning the video to an unstaggered trigger when this is necessary.

The storage of data in this map depends on the previous contents of the map in much the same way as was described in the section on the operation of the azimuth integrator. The difference is that, while in the case of the azimuth integrator the difference was multiplied by the integration constant, in the case of the scan storage, any difference in level simply changed the cell by one unit. This provided a small amount of scan-to-scan integration. It's primary purpose is to reduce the disturbance caused by a momentary high-level detection caused by a very strong aircraft target or similar phenomena. Additionally, the scan storage provides the means of synchronizing the input and output of the contour generator.

The input section was, as far as timing was concerned, completely independent of the output section. In other words, the input and output sections could be driven by different azimuth change pulses (ACP's), azimuth reference pulses (ARP's), and trigger pulses. This, among other things, provided the means for realignment of the displayed contour video. Also, any positional error caused by processing delays could be overcome simply by driving the contour generator with the same triggers, etc., as were used by the display being driven.

In an operational system, the data from this memory would be transmitted via phone lines or some other means to the indicator site. At this point, the information is read into a duplicate memory and used to generate the display.

The data are not directly read into or out of memory, but are first loaded into the memory controller along with the desired address. This is called a memory request. In the case of output from memory, the request does not contain data. The output data become available sometime before the next request is made. The request services are alternated whenever both an input and output request are made. The speed of the memory is much faster than the rate of requests, and so there is no possibility of missing either input or output requests. The timing for this circuit is shown in figure 14.

DEHOLING.

The operation of deholing is a discrete integration process designed to simulate the natural integration done by the eye on gray, level contours. This was particularly important in the generation of line contours which were not integrated by the eye. Figure 8 shows the simplified schematic of this device. It is basically a two-dimensional sliding window detector. The deholer received the three-bit video from the scan memory and immediately selected the contour level to be displayed. This thresholded information was processed serially in much the same manner as simple thresholded video. This one-bit video was delayed and sequenced to present the deholer area threshold section with nine bits of information representing a three-by-three array of weather cells. The following rules were applied to this array to generate another serial video bit stream: (1) If the center cell is empty, then do nothing; otherwise, total the surrounding cells, and (2) if the number of surrounding cells exceeds the preset deholer threshold, declare that the center cell and all of the eight surrounding cells contain weather; i.e., set them to one (refer to figure 15).

Notice that the minimum block size is now the three-by-three array. This had several consequences. First, all of the gaps and holes in the weather map were filled in or made smaller. Second, all of the isolated cells were removed. Third, some small amount of information was lost in the form of decreased resolution, but this is a natural consequence of the integration process. The output of the deholer is shown before contouring in figure 20. For comparison, figure 19 shows the same data with the deholer switched off. Notice that the great majority of small discontinuities have disappeared and that the edges which were jagged have been smoothed. This demonstrates the integration capability of the deholer circuitry. Also note that a larger hole can collapse to become a small hole. This is an unavoidable consequence of the deholing operation, but should not present any problems, because it is still an accurate presentation of the actual weather being detected.

CONTOUR GENERATION.

It was advantageous to generate the different required contours with the same equipment and, if at all possible, with the same technique. This was the principal reason the symbolic representation technique described earlier was chosen. The implementation of this technique will now be discussed with reference to the simplified schematic in figure 9.

The incoming video from the deholer was sequenced into a three-by-three array in exactly the same manner as in the deholer just described. The array was then examined by the decision ROM to determine which of the 16 symbols of the chosen contour type should be displayed in the location at the center of the three-by-three array. This is accomplished for each range-azimuth cell of the display. This decision was accomplished independently of the countour type at this point because of the restrictions in the types of symbols that could be used to generate contours. This is described in detail in appendix B. In addition, this appendix also contains the contents of the decision ROM with the address given as a three-by-three array.

The sequence of symbols to be generated was saved in the symbol shift register for the entire duration of the display cell. This information was fed to the contour symbol generator which consisted of the symbol table ROM and an output shift register. The contents of the symbol ROM is also shown in appendix B.

A total of four, 16-symbol sets was stored in each ROM, and each symbol consisted of an eight-by-eight array of dots. The outputs of each contour generator were then sent to the mixer where they were all combined and outputted to the display. The final system output for several cases is shown in figures 21 through 28. Because the symbol set can be modified by changing the contents of a single ROM and because the programing effort is almost trivial, this device would make an ideal test bed for the development and test of other contouring formats.

The line contours do not become objectionable until the map information is introduced. In areas where map information is not complicated or congestive, the line contours may be preferable, but in areas where the map information

is complicated, the gray, shaded contours are to be preferred. Probably both of these contours should be offered to suit the controllers' preference. The dots in contour type 3 would be very helpful when the weather extends off the screen, because it would better indicate the weather position. It was not observed that the shaded levels had a detrimental effect on the detection of weak radar targets in weather and, in fact, may have enhanced their detectability.

CONCLUSIONS

1. The subject weather-contouring device is usable for ATC purposes and meets the requirements specified for this project.

2. The accuracy of the total weather detection system was not limited by the contour device or the averaging that was done. The most severe limitations result from the inherent characteristics of the radar.

3. A measurement resolution of 0.8 nmi and 16 or 32 effective azimuth samples provided sufficient samples for an ASR-type radar to enable the contour device to generate useful contours.

4. The display resolution of the contour device was 0.4 nmi by 16 ACP (1.4°). This provided sufficient detail for high-quality contour presentation and, at the same time, provided sufficient coarseness for proper action of the deholer circuitry.

5. The threshold of detection can be set to within 1 dB if 60-dB log normal video is used as the input. This accuracy is well within the uncertainty of measurement for ASR radars and poses no threat of significantly inaccurate measurements.

6. The use of the deholer circuitry significantly improves the quality of the resultant display.

7. The contour generator effectively contours weather, and because it is programmable, the display format can be readily changed. The realignment feature eliminates the problems due to azimuth and range shifting, common in the earlier contouring systems.

RECOMMENDATIONS

1. It is recommended that the subject weather-contouring device be considered for implementation whenever a PPI display is to be used.

2. It is also recommended that this technique be investigated to determine if it has applications in the all-digital environment, including conversion of the algorithms used to provide a random write (vector) display output.

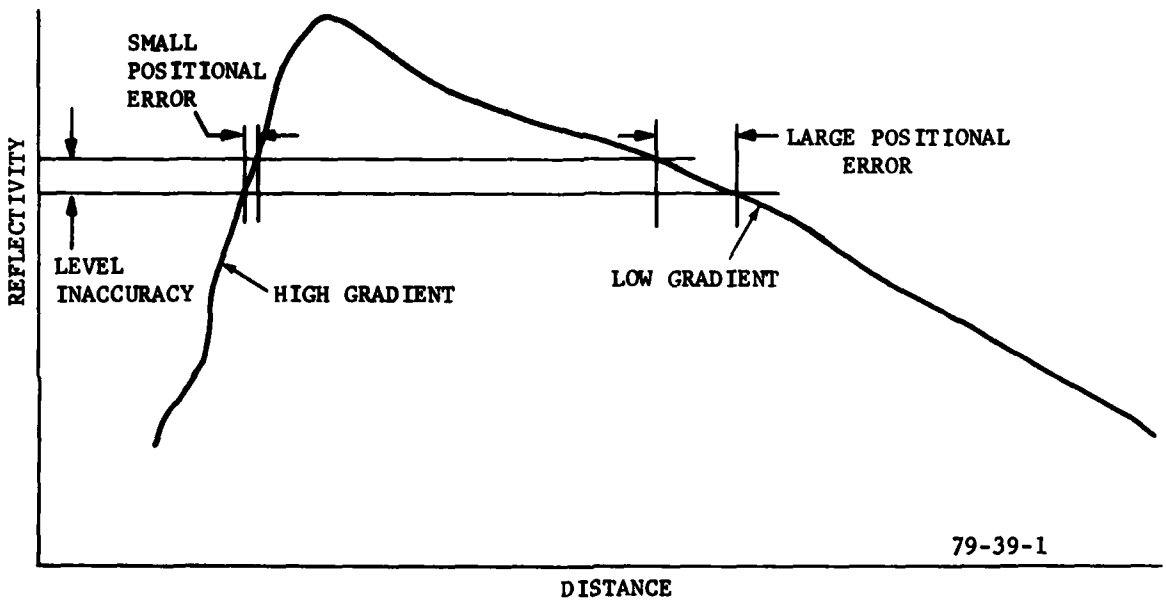

FIGURE 1. THE EFFECT OF REFLECTIVITY GRADIENT ON POSITIONAL AND LEVEL ACCURACY

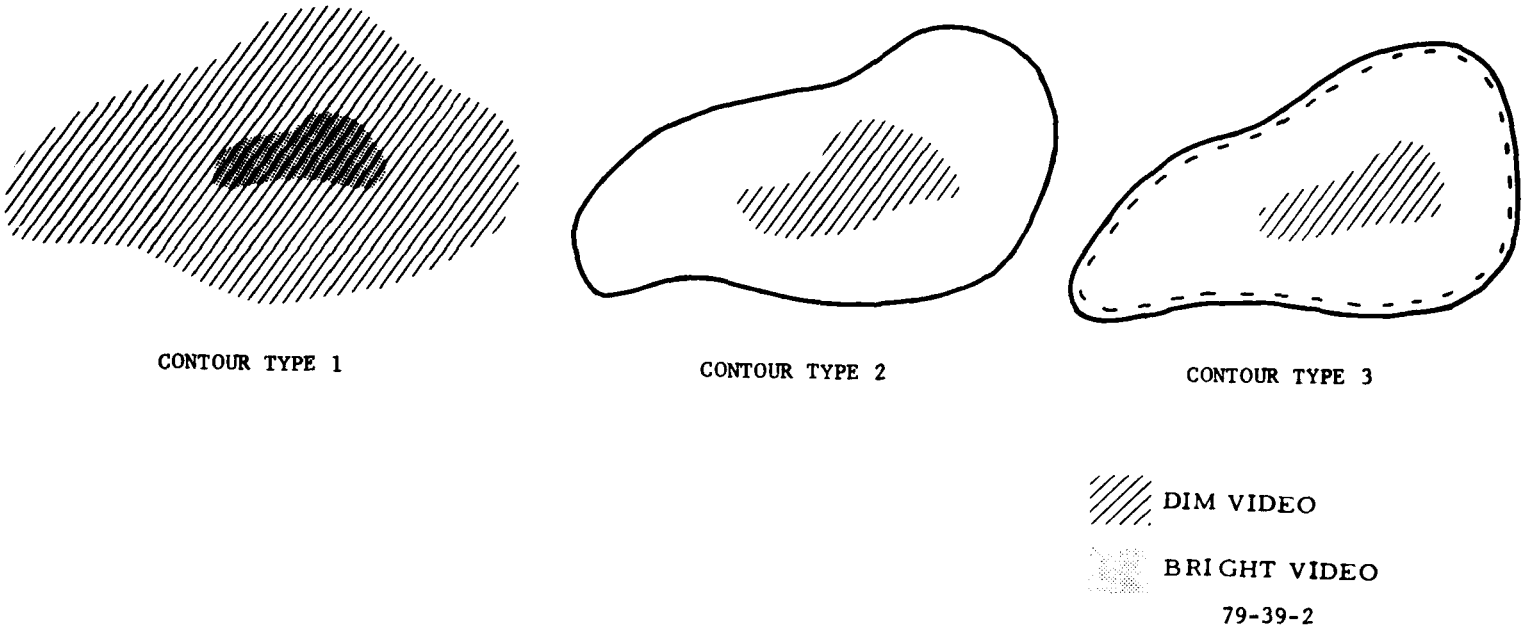

FIGURE 2. PROPOSED CONTOUR TYPES

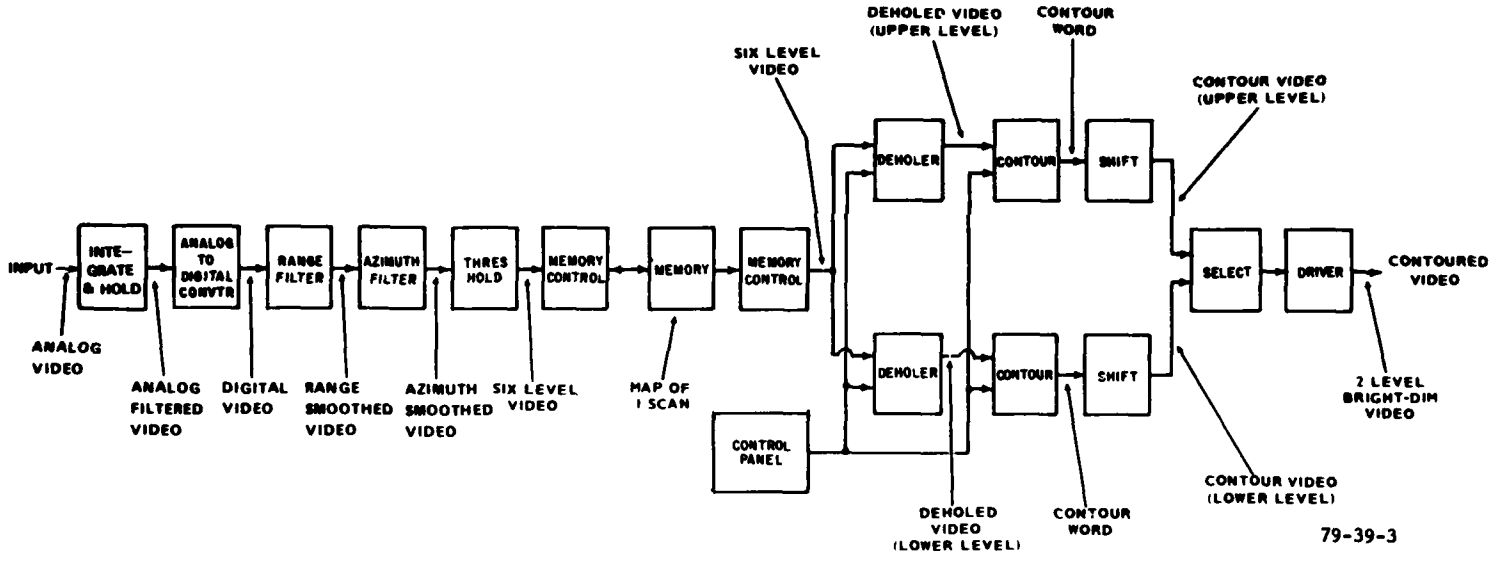

FIGURE 3. SYSTEM BLOCK DIAGRAM

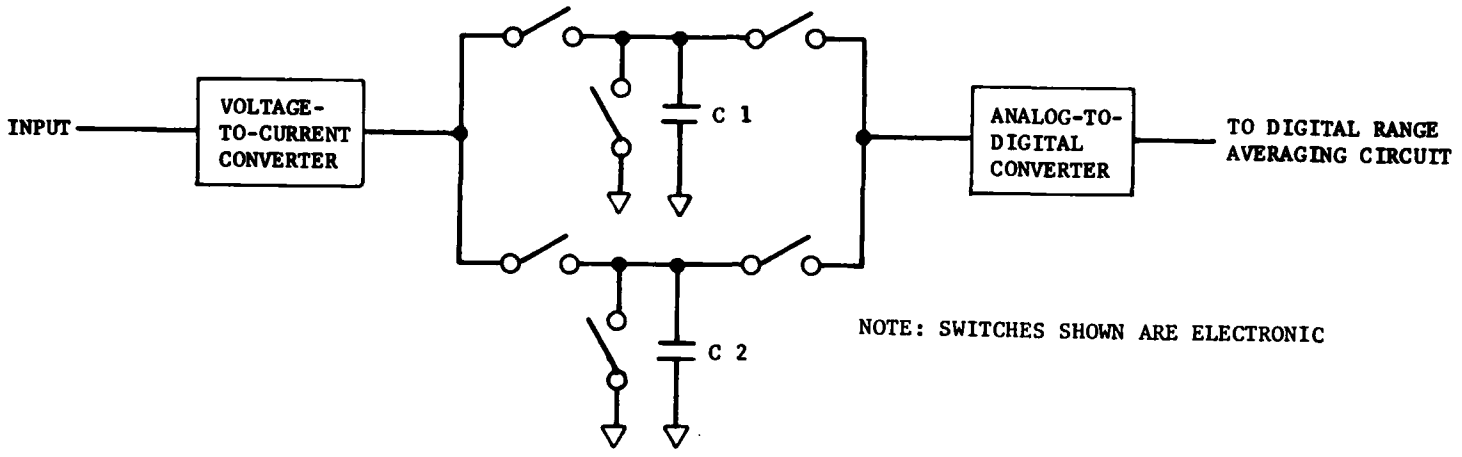

A. ANALOG RANGE AVERAGING

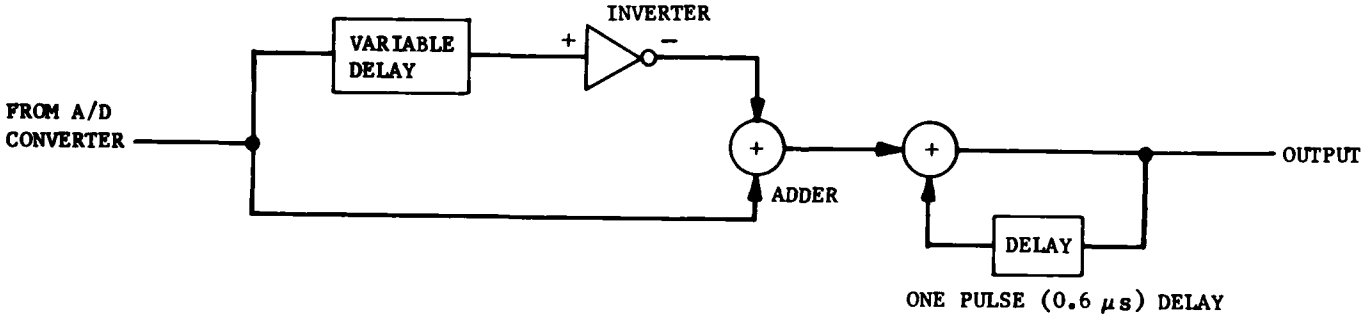

B. DIGITAL RANGE AVERAGING

79-39-4

FIGURE 4. RANGE AVERAGING SCHEMATIC DIAGRAMS

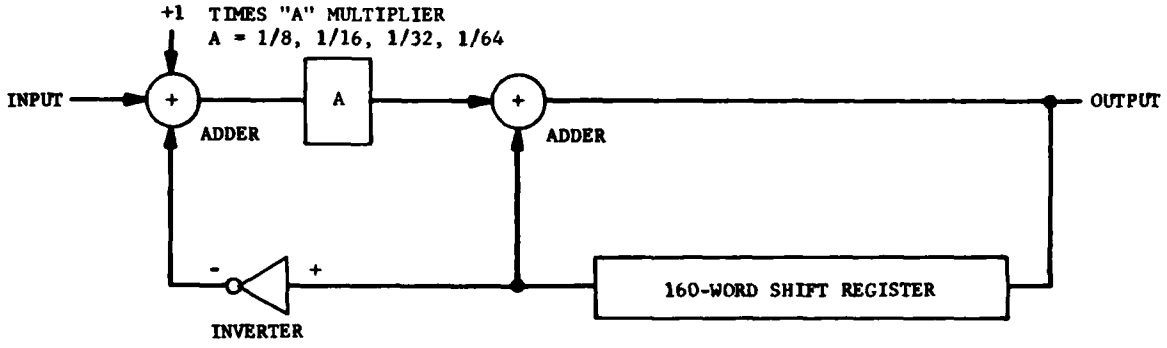

FIGURE 5. AZIMUTH AVERAGING SCHEMATIC DIAGRAM

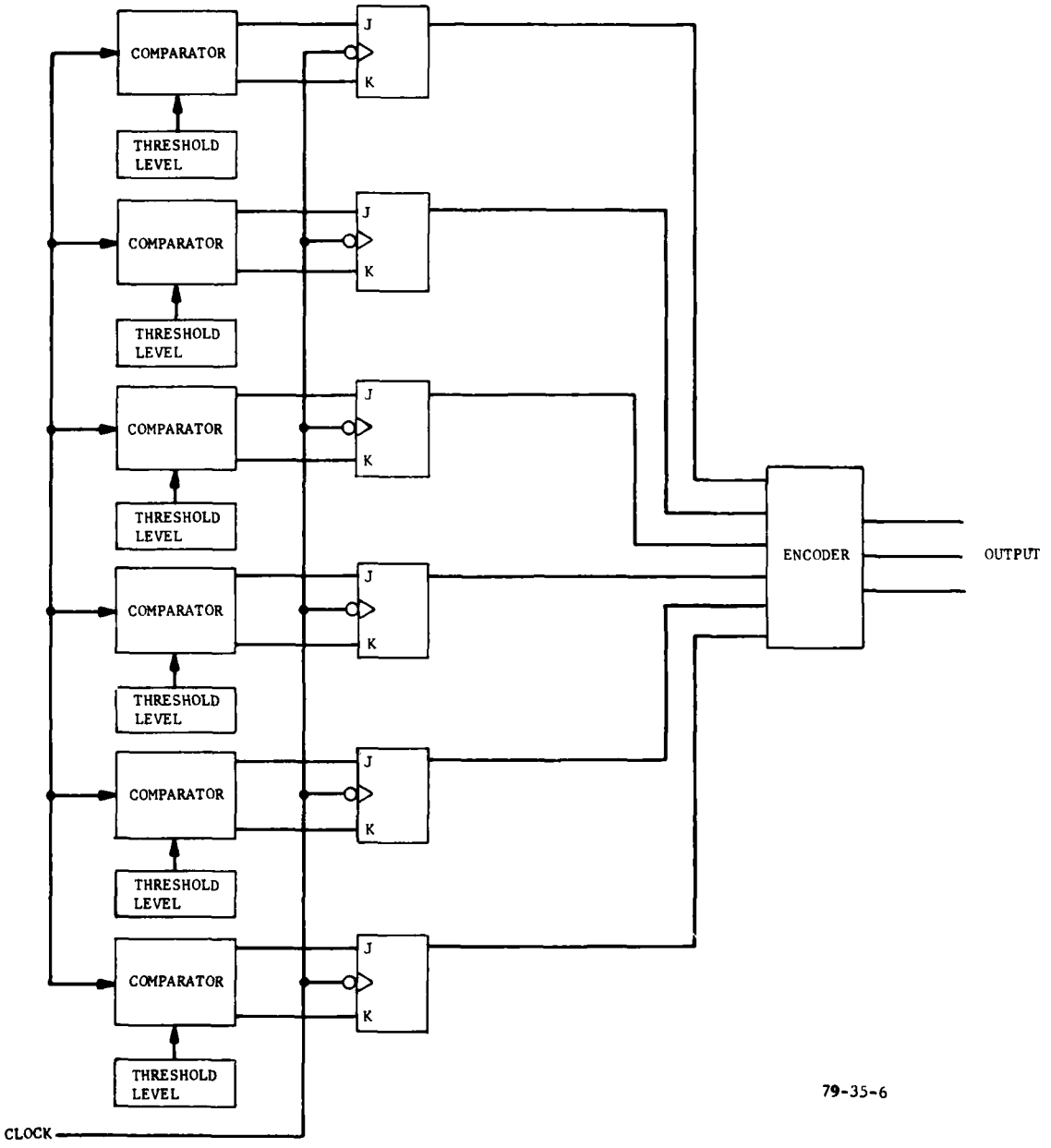

FIGURE 6. THRESHOLDING CIRCUIT SCHEMATIC DIAGRAM

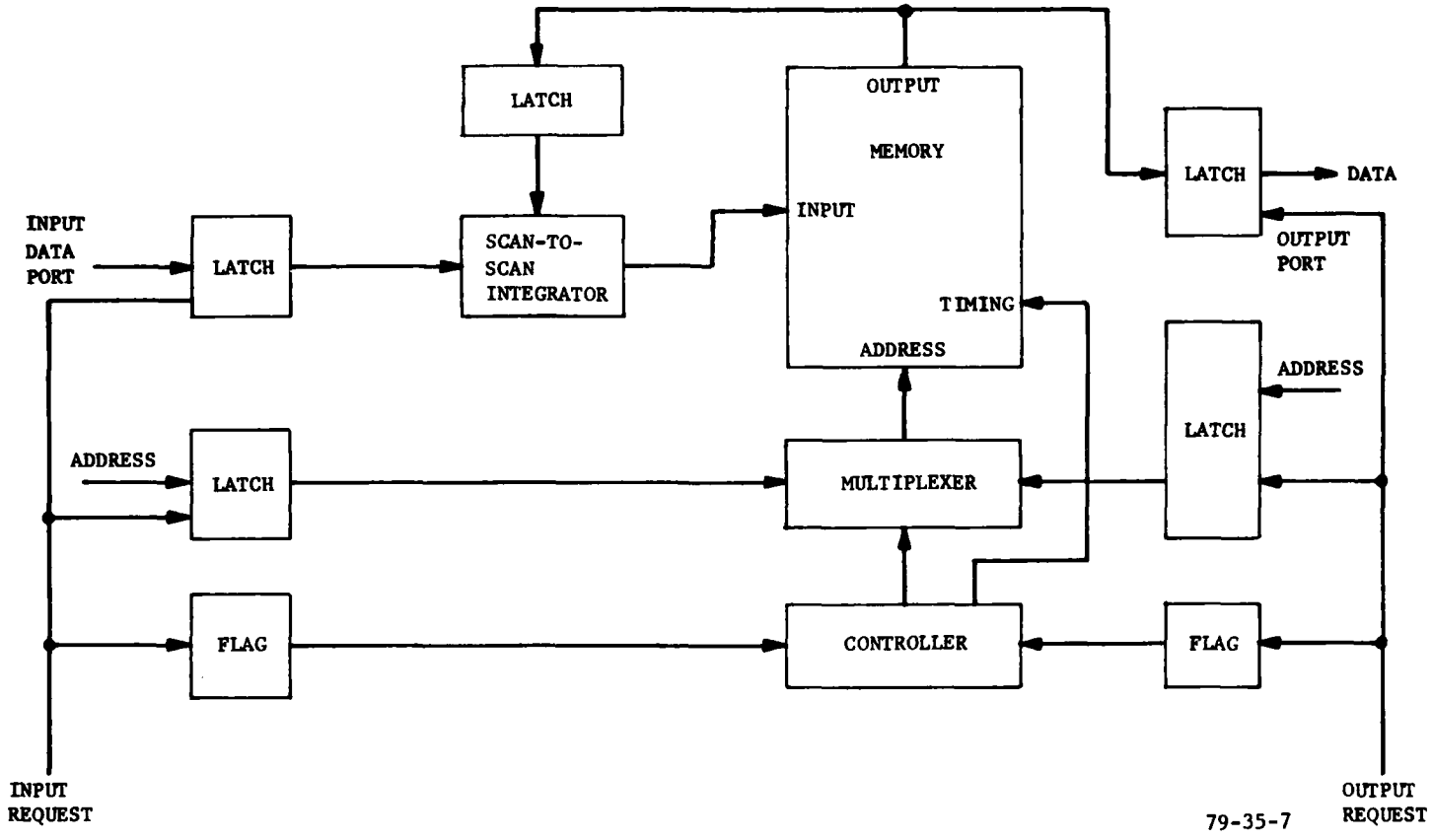

FIGURE 7. SCAN STORAGE MEMORY CONTROLLER SCHEMATIC DIAGRAM

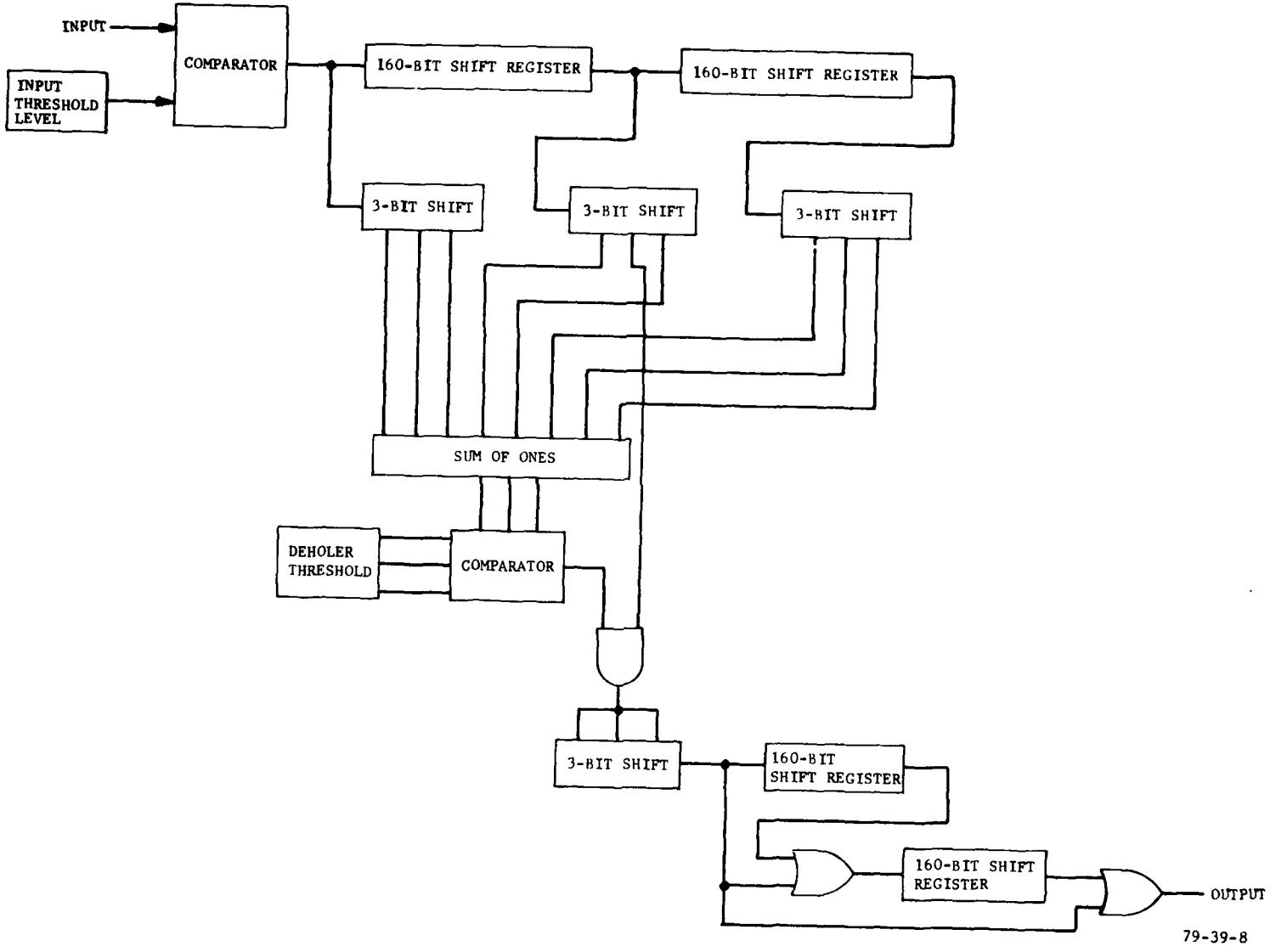

FIGURE 8. DEHOLER SCHEMATIC DIAGRAM

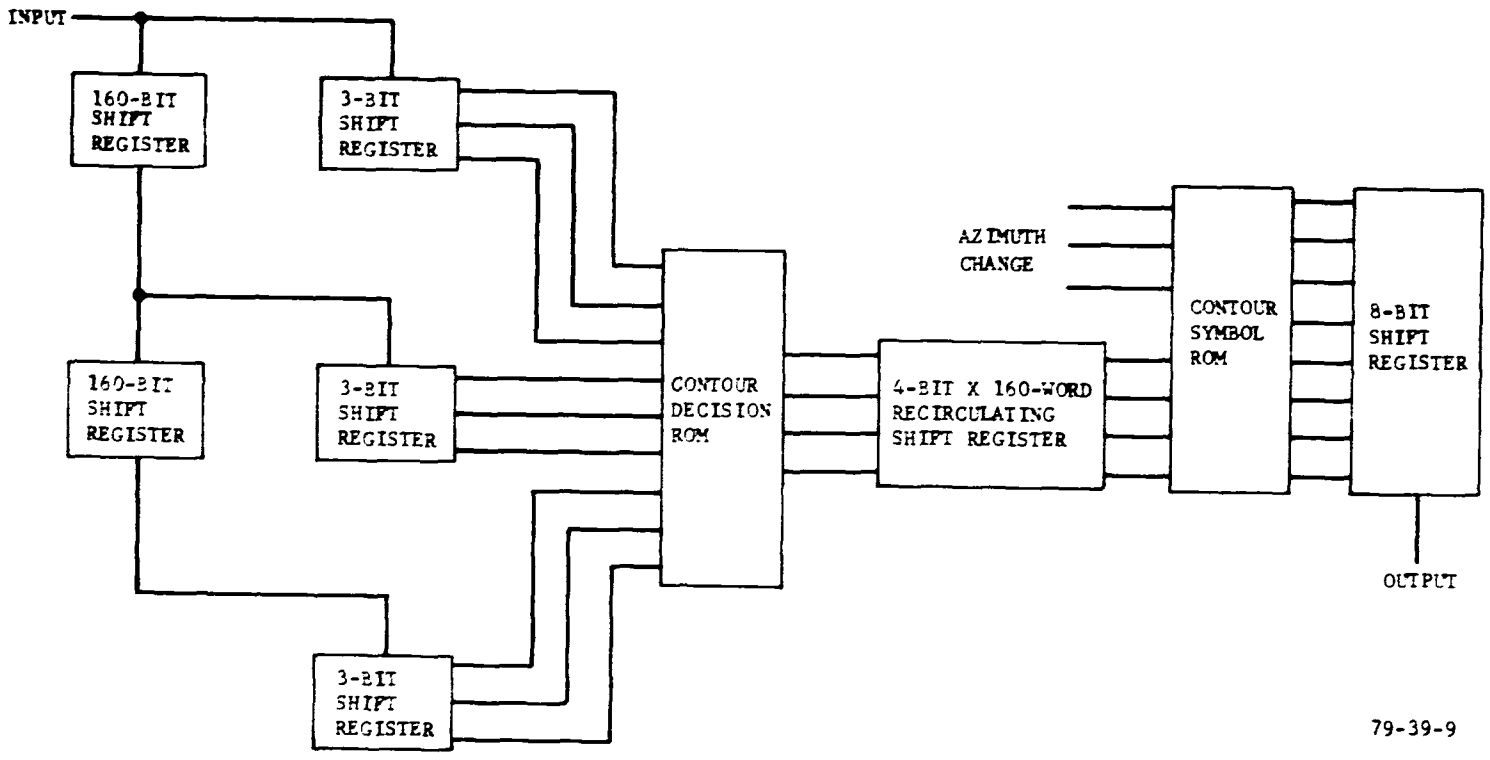

FIGURE 9. CONTOUR GENERATOR SCHEMATIC DIAGRAM

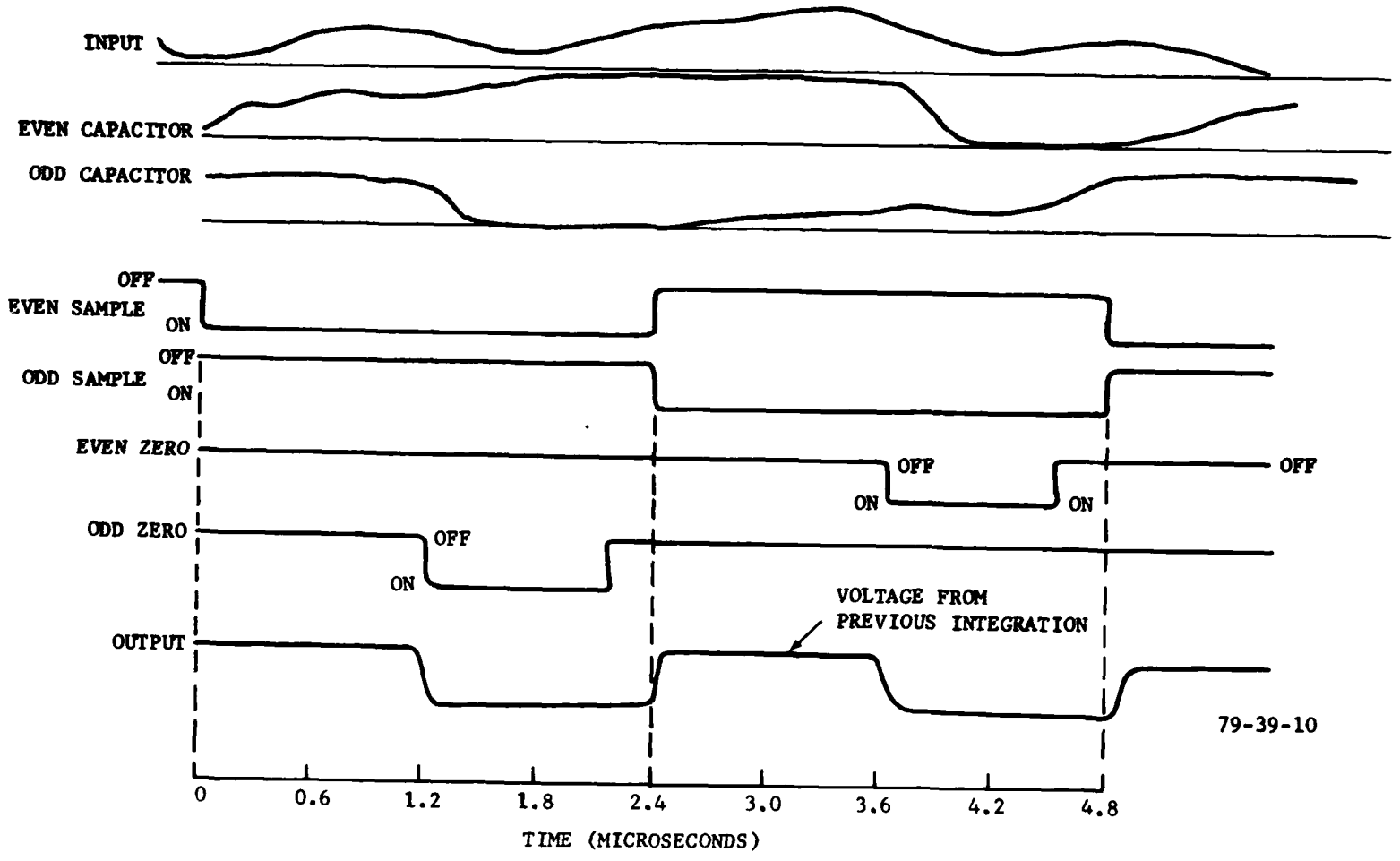

FIGURE 10. ANALOG AVERAGING TIMING

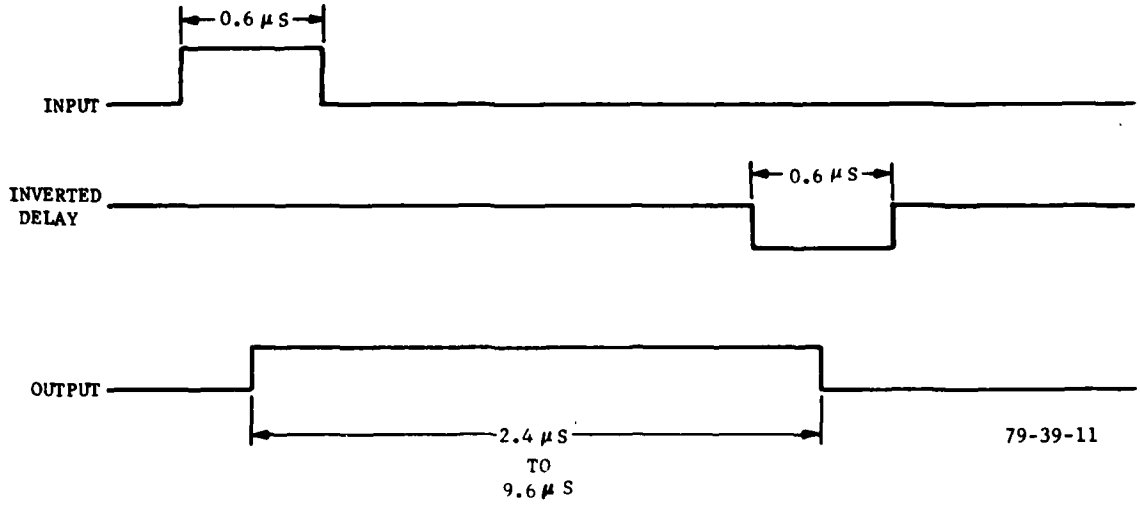

FIGURE 11. DIGITAL AVERAGING TIMING

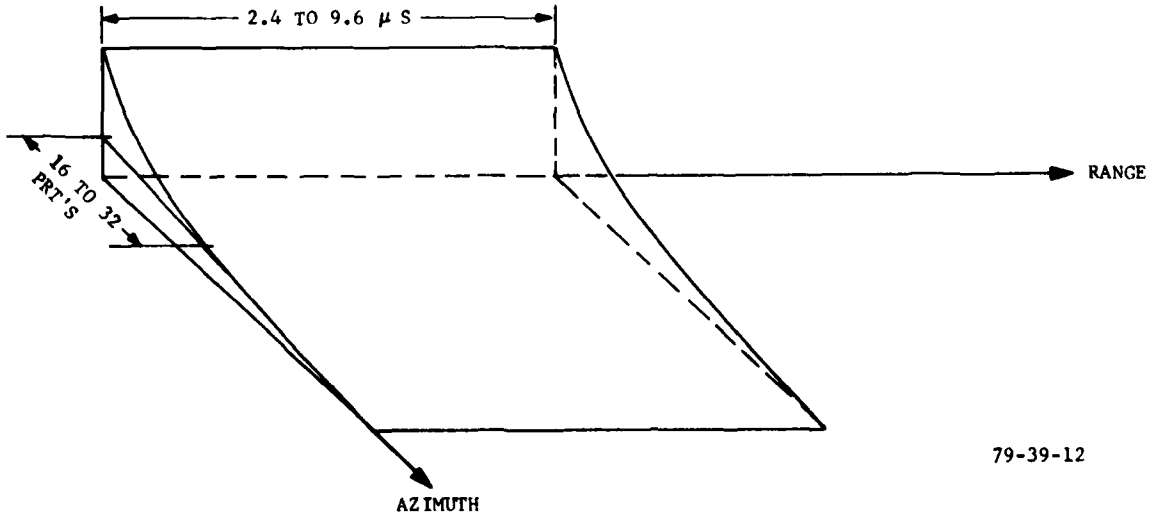

FIGURE 12. RANGE AND AZIMUTH COMPOSITE WEIGHTING FUNCTION

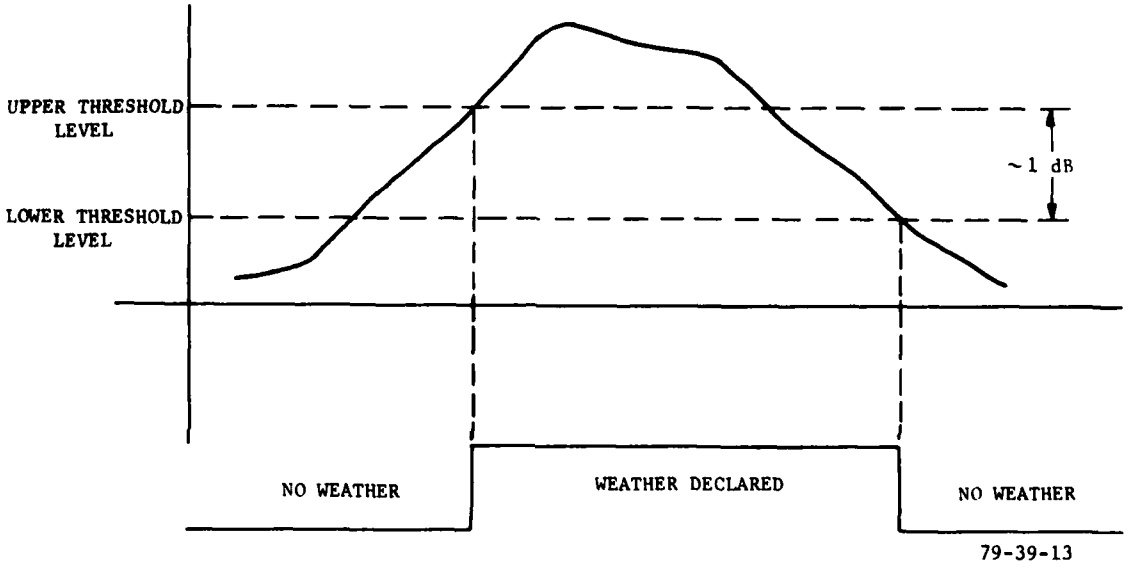

FIGURE 13. THRESHOLD CIRCUIT HYSTERESIS

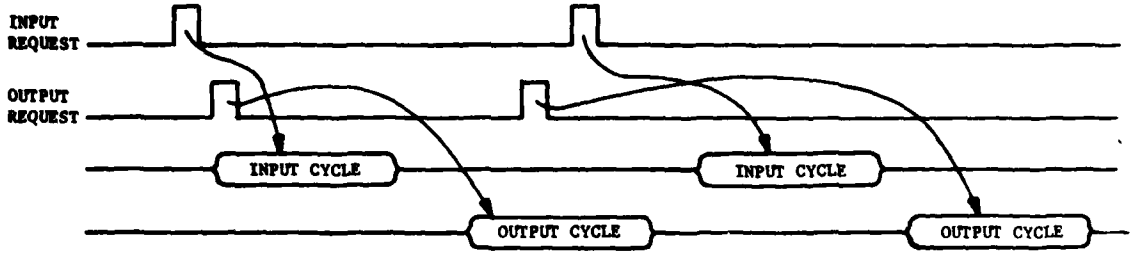

- WHEN BOTH REQUESTS ARE PENDING AT THE COMPLETION OF A CYCLE, THE ALTERNATE TYPE (INPUT, OUTPUT) OF CYCLE IS INITIATED.

- INPUT AND OUTPUT REQUESTS ARE ASYNCHRONOUS

79-39-14

FIGURE 14. MEMORY CONTROLLER TIMING

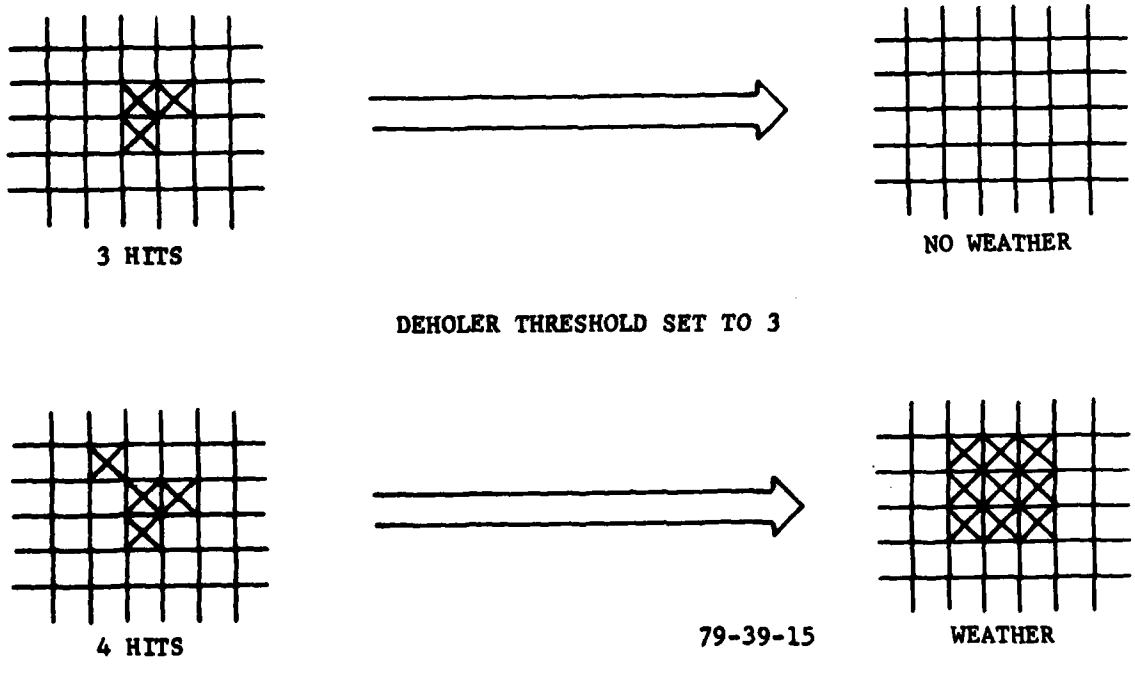

FIGURE 15. DEHOLER OPERATION

FIGURE 16. RESULT OF RANGE AVERAGING

FIGURE 17. RESULT OF AZIMUTH AVERAGING

FIGURE 18. RESULT OF THRESHOLDING

FIGURE 19. RESULT OF PROCESSING SHOWN BEFORE DEHOLING

FIGURE 20. RESULT OF PROCESSING SHOWN AFTER DEHOLING

FIGURE 21. SYSTEM OUTPUT, CONTOUR TYPE 1, DEHOLER ON

FIGURE 22. SYSTEM OUTPUT, CONTOUR TYPE 2, DEHOLER ON

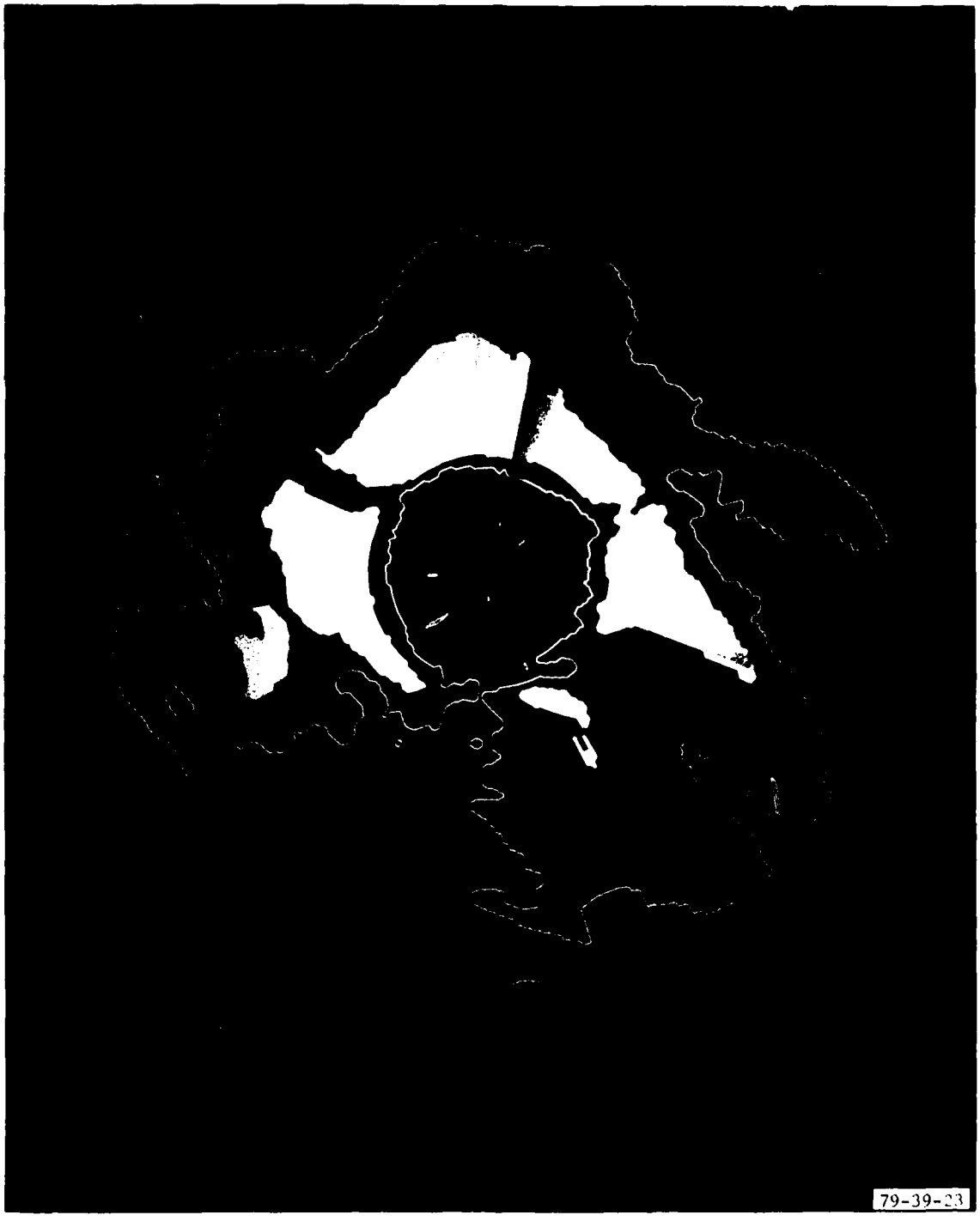

FIGURE 23. SYSTEM OUTPUT, CONTOUR TYPE 3, DEHOLER ON

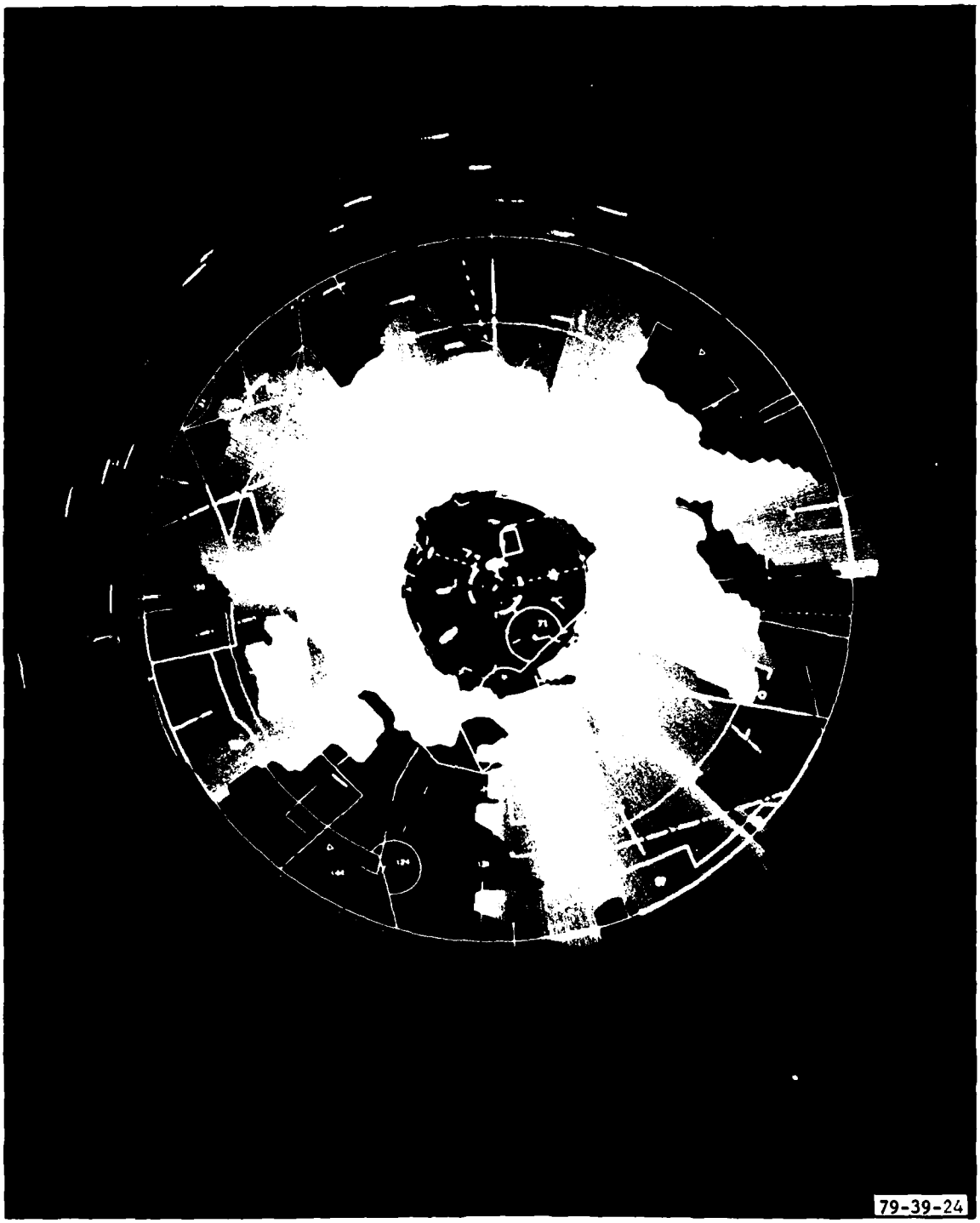

FIGURE 24. SYSTEM OUTPUT, CONTOUR TYPE 1, WITH MAP

FIGURE 25. SYSTEM OUTPUT, CONTOUR TYPE 3, WITH MAP

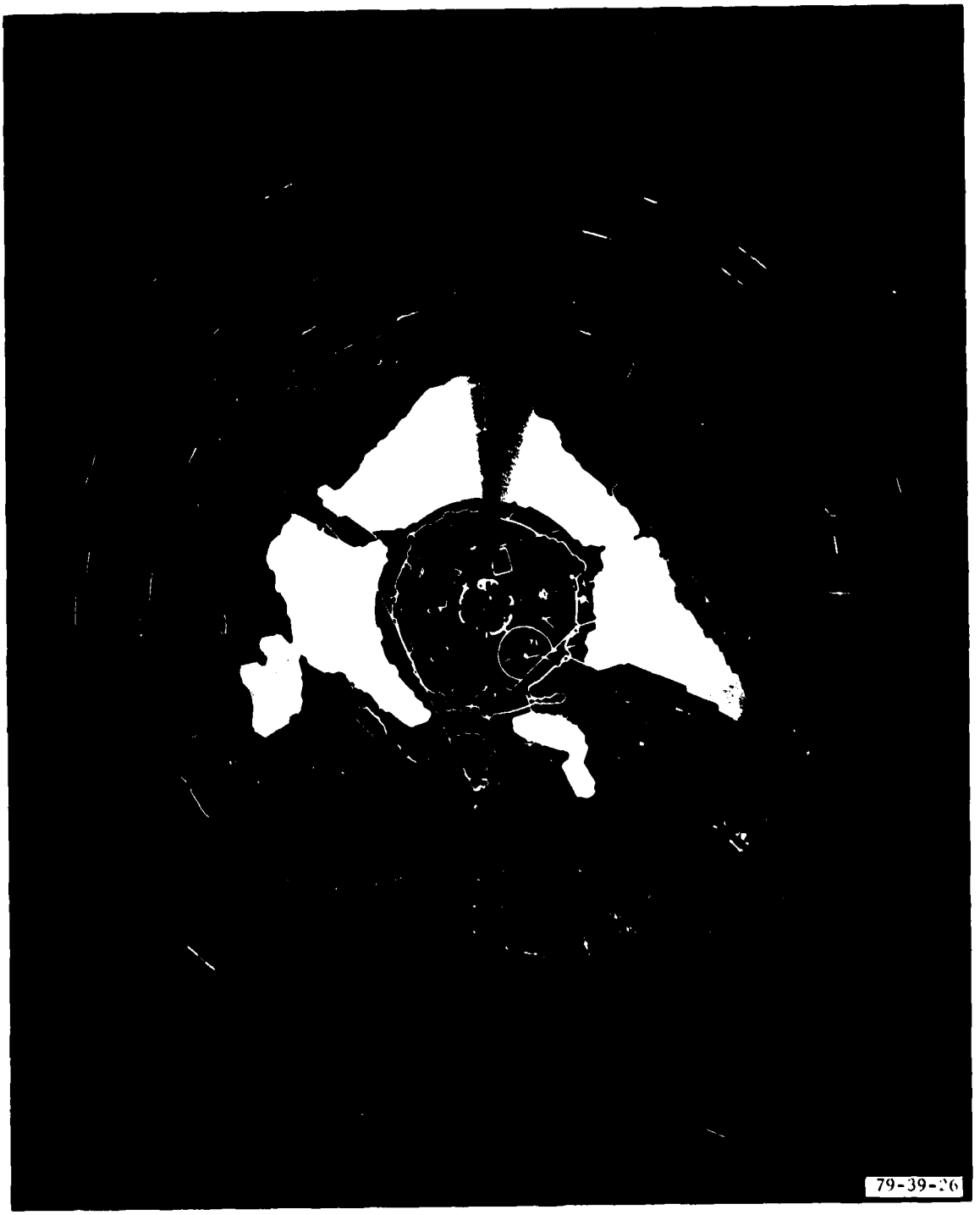

FIGURE 25. SYSTEM OUTPUT, CONTOUR TYPE 3, WITH MAP

FIGURE 27. SYSTEM OUTPUT, CONTOUR TYPE 2, WITH RAW WEATHER

FIGURE 28. SYSTEM OUTPUT, CONTOUR TYPE 3, WITH RAW WEATHER

APPENDIX A

CALCULATIONS OF SIGNAL-TO-NOISE RATIO IMPROVEMENT DUE TO AVERAGING IN RANGE AND AZIMUTH

The signal-to-noise improvement (defined as the ratio of the variance of the averaged signal to the variance of the original signal) resulting from range averaging a weather signal is, because the range samples are measurements of independent sample volumes, equal to the number of samples averaged. When 16 samples are averaged, the signal-to-noise ratio increases by a factor of 16. Since the variance of log normal weather video is 31 dB^2 without averaging, the variance of the average will be 1.94 dB^2, and the root mean square (RMS) noise will be 1.4 dB.

The samples in a given range cell are partially correlated with time; that is, they are not independent. What decorrelation exists results from two major sources: the scanning of the antenna beam and the motion of raindrops within the sample volume.

The beam shape autocorrelation function is computed by assuming a Gaussian shaped antenna beam (figure A-1). The attenuation pattern for a Gaussian-shaped beam is given by

$$A = \exp\left\{-\theta^2/2\phi^2\right\}$$

where: A is the two-way voltage gain
θ is the angle off beam center
ϕ is a constant related to the beam width

expressed in dB this becomes

$$20 \log A = 20 \log \left(\exp\left\{-\theta^2/2\phi^2\right\}\right)$$

$$= (\theta^2/2\phi^2)\ 20 \log e$$

$$= (\theta^2/\phi^2)\ 4.34$$

when $\theta = 1/2\,\gamma$ (γ is the two-way beamwidth) the attenuation is, by definition, 3 dB, so

$$-3 = (\theta^2/\phi^2)\ 4.34 = (1/2\,\gamma)^2/\phi^2\ 4.34.$$

Solving for ϕ in terms of γ yields

$$\phi^2 = .36\gamma^2$$
$$\phi = .6\gamma.$$

Now, for the case of the ASR-8 radar, $\gamma = 1°$ or 1.75×10^{-2} radians. So,

$$A = \exp -\left\{\theta^2/2 \bullet .36 \bullet \left[1.75 \times 10^{-2}\right]^2\right\}$$

$$A = \exp -\left\{\theta^2(4.56 \times 10^3)\right\}.$$

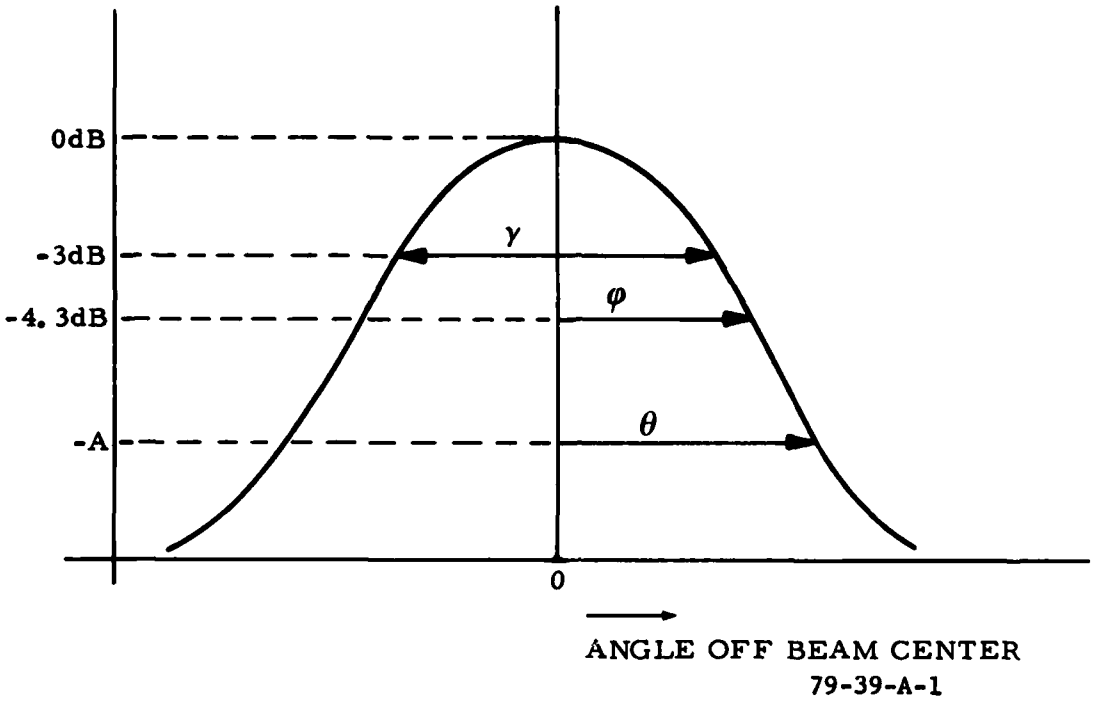

FIGURE A-1. TWO-WAY ATTENUATION VERSUS ANGLE OFF BEAM CENTER

The antenna rotates at a constant velocity, w, so A is a function of time.

$$\theta = wt = (2\pi/\text{rev})(12\ \text{rev/min})(1\ \text{min}/60\ \text{sec})t$$

$$\theta = 1.26t$$

$$\theta^2 = 1.58t^2$$

so

$$A = \exp\left\{-1.58t^2\ [4.5\text{x}10^3]\right\}$$

$$= \exp -\left\{[7.23\text{x}10^3]t^2\right\}.$$

The Fourier transform of this function yields

$$F\{A\} = (\pi/7.23\ H0^3)^{1/2} \exp\left\{-w^2/4 \text{ x } 7.23\text{x}10^{-5}\right\}$$

$$= 2.08\text{x}10^{-2} \exp\left\{-w^2\ 3.46\text{x}10^{-5}\right\}.$$

The power spectral density is therefore given by

$$S(w) = 4.34\text{x}10^{-4} \exp\left\{w^2 \quad 6.92\text{x}10^{-5}\right\}.$$

The 3-dB bandwidth is given by

$$1/2 = \exp -\left\{ w^2 \; 6.92\text{x}10^{-5}\right\}$$

$$w^2 = (\ln 2)/6.92\text{x}10^{-5} = 1\text{x}10^4$$

$$w = 100 = 2\pi f$$

$$f = 100/2\pi = 15.9 \text{ Hz.}$$

The beam-shape autocorrelation is thus,

$$R(\tau) = 1.47\text{x}10^{-2} \exp\left\{-3.62\text{x}10^3 \tau^2\right\}.$$

The composite variance for a weather echo is due mostly to turbulence and shear and was given by Sirmans and Doviak (reference 1) as $\sigma_v^2 = \sigma_t^2 + \sigma_s^2$ where σ_v^2 is the total variance, σ_t^2 is the variance due to turbulence, and σ_s^2 is the variance due to shear.

$$\sigma_s^2 = [.42 \; \text{KvR}\theta_2 \cos\theta_e]^2 \text{ m}^2/\text{sec}$$

$$\sigma_t^2 = 2 \text{ m}^2/\text{sec approx.}$$

where	$\text{Kv} = 4\text{x}10^{-3} \text{ sec}^{-1}$	shear constant
	$\text{R} = 20 \text{ nmi} = 3.22\text{x}10^4\text{m}$	range
	$\theta 2 = 5°$	two-way vertical beamwidth
	$\theta e = 0°$	elevation angle

$$\sigma_s^2 = 22.3 \text{ m}^2/\text{sec}^2$$

$$\sigma_v^2 = 24.3 \text{ m}^2/\text{sec}^2$$

$$\sigma_v = 5 \text{ m/sec.}$$

σ_v is transformed into frequency by the Doppler equation by

$$\sigma fv = \frac{2\sigma v\, f_o}{C} = \frac{2 \times 5 \times 2.9\times10^9}{3 \times 10^8} = 96 \text{ Hz} .$$

Assuming a Gaussian-shaped power spectral density, this becomes

$$S_w(w) = e^{-w^2/2}\ [607]^2$$

so $$R(\tau) = \frac{1.84\times10^5}{\pi}\ e^{-[1.85\times10^5]\tau^2}.$$

The autocorrelation of the weather signal is

$$R_{ww}(\tau) = w\ e^{-\tau^2}1.85\times10^5,$$

and the autocorrelation of the beam shape is

$$R_{ss}(\tau^2) = Be^{-\tau^2}3.62\times10^3.$$

The composite correlation is then

$$R_{ss}(\tau) = R_{ww}(\tau)R_{BB}(\tau) = WBe^{-\tau^2[1.89\times10^5]}.$$

When this is filtered by the azimuth integrater, the output spectrum is given by $S_o(w) = S_s(w)H_a(w)H^*_a(w)$.

The resulting correlation function is, with $\tau = nT$

$$R_{oo}(n\tau) = R_{ss}(n\tau)\ [h_a(n) * h_a(n)].$$

The bracketed term is given by

$$h_a(\tau) \times h_a(\tau) = \frac{1}{N} \sum_{k=o}^{N} a[1-a]^k\ a[1-a]^{n-k}$$

$$= \frac{N}{N} a^2[1-a]^n = a^2[1-a].$$

Using the results of appendix C, the h(n) x h(n) term becomes

$$h(n) \times h(n) = \frac{1}{N} \sum_{k=o}^{N} a[1-a]^k\ a[1-a]^{n-k}$$

$$= a^2[1-a].$$

The filtered signals autocorrelation is given by

$$R_{oo}(nT) = R_{ss}(nT) \times a^2[a-1]^n$$

$$\sigma_o^2 = R_{oo}(o) = \frac{1}{N} \sum_{k=o}^{N} R_{ss}(kT)\ a^2[1-a]^{n-k} \Bigg|_{n\,=\,o}$$

$$= \frac{1}{N} \sum_{k=o}^{N} e^{-[kT]^2}\ 1.89\times10^5\ a^2[1-a]^{-k}$$

$$= \frac{a^2}{N} \sum_{k=o}^{N} e^{-.18k^2}\ [1-a]^{-k}.$$

When $a = \frac{1}{8}$ (i.e., the smallest time constant used)

$$\sigma_o^2 \doteq \frac{1}{64}\ \frac{1}{N}\ [1 + .95 + .64 + .30 + .1 + .02\ .\ .\ ]$$

$$\sigma_o^2 = \frac{1}{64} \times \frac{1}{6} \times 3.01 = \frac{1}{128}.$$

For the case of noise (where the autocorrelation is 1 at n=o and o elsewhere)

$$\sigma_n^2 = \frac{1}{64} \times \frac{1}{6} \times 1 = \frac{1}{384}$$

$$\frac{\sigma_n^2}{\sigma_o^2} = \frac{1}{3}\ .$$

Hence, the number of independent samples is roughly one-third the number of actual samples. The total number of independent samples is thus $\frac{1}{3} \times 16 \times 16 = 85$, and so the resultant variance will be decreased to $\frac{31\ dB^2}{85} = 0.36\ dB$.

REFERENCE

1. Sirmans, D., and Doviak, R. J., Meteorological Radar Signal Intensity Estimation, National Oceanic and Atmospheric Administration, TM ERL NSSL-64, 1973.

APPENDIX B

CONTOUR GENERATOR ROM PROGRAMING

A three-by-three matrix represented by a nine-bit number is fed into the character decision ROM.

8	7	6	5	4	3	2	1	0

The nine-bit number represents the matrix as follows

8	7	6
5	4	3
2	1	0

The leftmost three bits represent the top row of the three-by-three matrix, the center three bits represent the center row, and the rightmost three bits represent the bottom row.

If any of the bits are a logical "1," the cell is "filled," showing that weather is present. For example, if the binary number 111 010 101 were inputted to the character decision ROM, it would represent the following matrix:

111 010 101 ⟶

1	1	1
0	1	0
1	0	1

⟶ 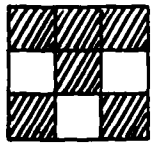

The purpose of the character decision ROM is to assign one of 16 characters to each of the three-by-three matrices, of which there are 512 possibilities. These are all listed in the following eight pages. Below each of the matrices is the three-digit octal number that represents it (000_8 - 777_8).

Below the octal number representing the matrix is a hexadecimal number. This number represents the character that corresponds to weather in that matrix. This number is outputted from the character decision ROM into the character generator ROM. The character generator ROM outputs an eight-by-eight matrix which is displayed as a character representing weather in the original three-by-three matrix.

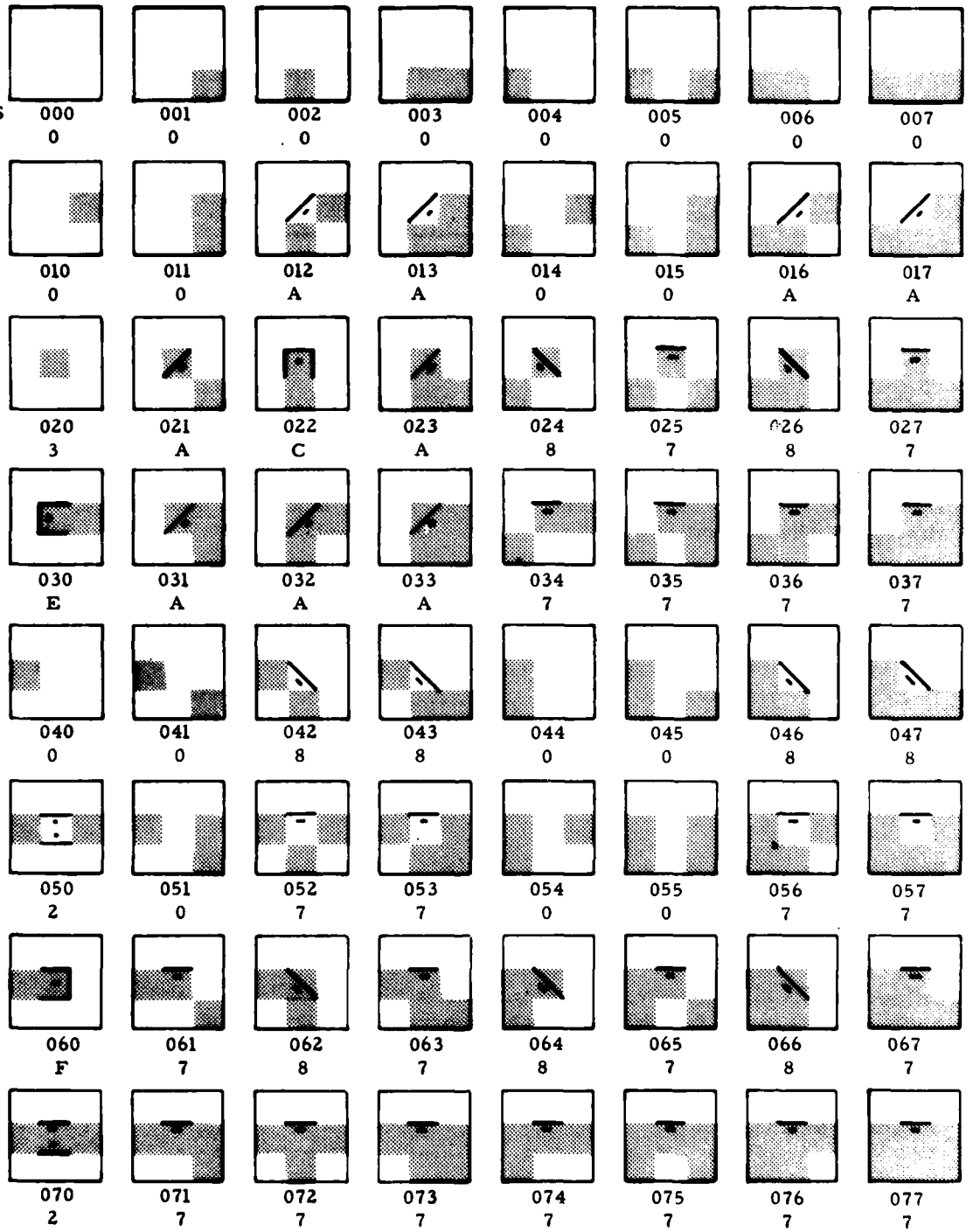
ADDRESS
OUTPUT
000 0
001 0
002 0
003 0
004 0
005 0
006 0
007 0
010 0
011 0
012 A
013 A
014 0
015 0
016 A
017 A
020 3
021 A
022 C
023 A
024 8
025 7
026 8
027 7
030 E
031 A
032 A
033 A
034 7
035 7
036 7
037 7
040 0
041 0
042 8
043 8
044 0
045 0
046 8
047 8
050 2
051 0
052 7
053 7
054 0
055 0
056 7
057 7
060 F
061 7
062 8
063 7
064 8
065 7
066 8
067 7
070 2
071 7
072 7
073 7
074 7
075 7
076 7
077 7

79-39-B-1

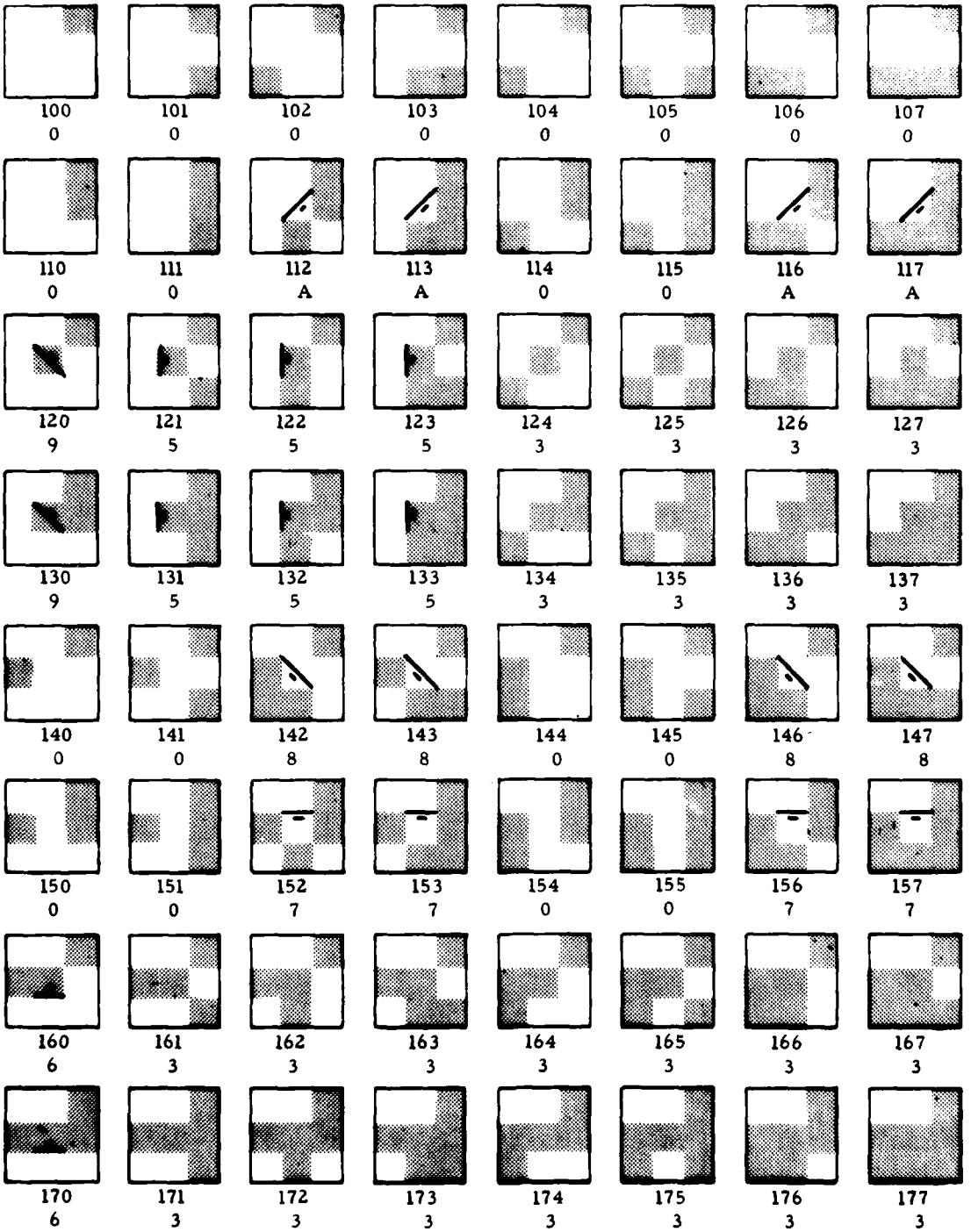
100 0
101 0
102 0
103 0
104 0
105 0
106 0
107 0
110 0
111 0
112 A
113 A
114 0
115 0
116 A
117 A
120 9
121 5
122 5
123 5
124 3
125 3
126 3
127 3
130 9
131 5
132 5
133 5
134 3
135 3
136 3
137 3
140 0
141 0
142 8
143 8
144 0
145 0
146 8
147 8
150 0
151 0
152 7
153 7
154 0
155 0
156 7
157 7
160 6
161 3
162 3
163 3
164 3
165 3
166 3
167 3
170 6
171 3
172 3
173 3
174 3
175 3
176 3
177 3

79-39-B-2

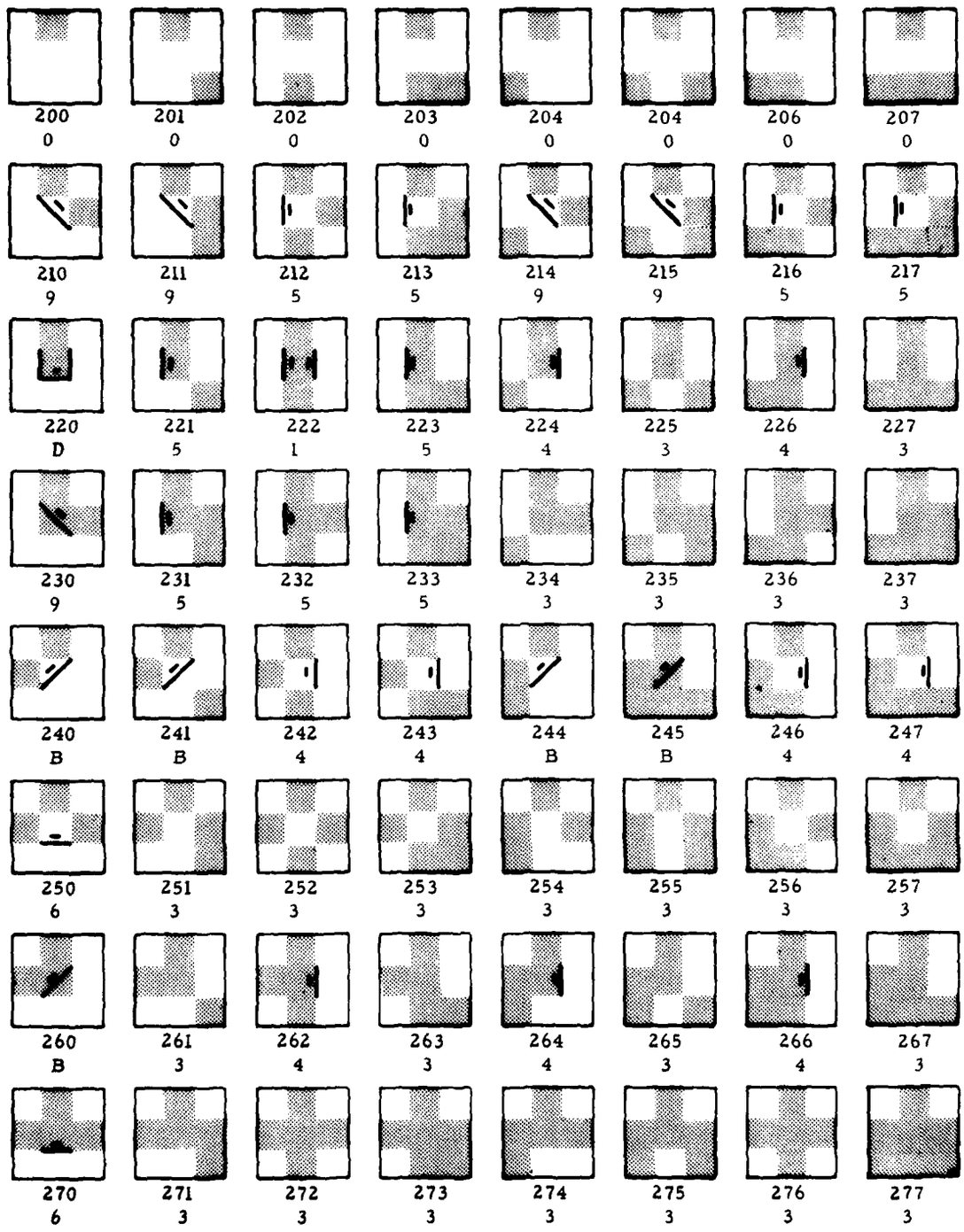
200
0
201
0
202
0
203
0
204
0
204
0
206
0
207
0
210
9
211
9
212
5
213
5
214
9
215
9
216
5
217
5
220
D
221
5
222
1
223
5
224
4
225
3
226
4
227
3
230
9
231
5
232
5
233
5
234
3
235
3
236
3
237
3
240
B
241
B
242
4
243
4
244
B
245
B
246
4
247
4
250
6
251
3
252
3
253
3
254
3
255
3
256
3
257
3
260
B
261
3
262
4
263
3
264
4
265
3
266
4
267
3
270
6
271
3
272
3
273
3
274
3
275
3
276
3
277
3

79-39-B-3

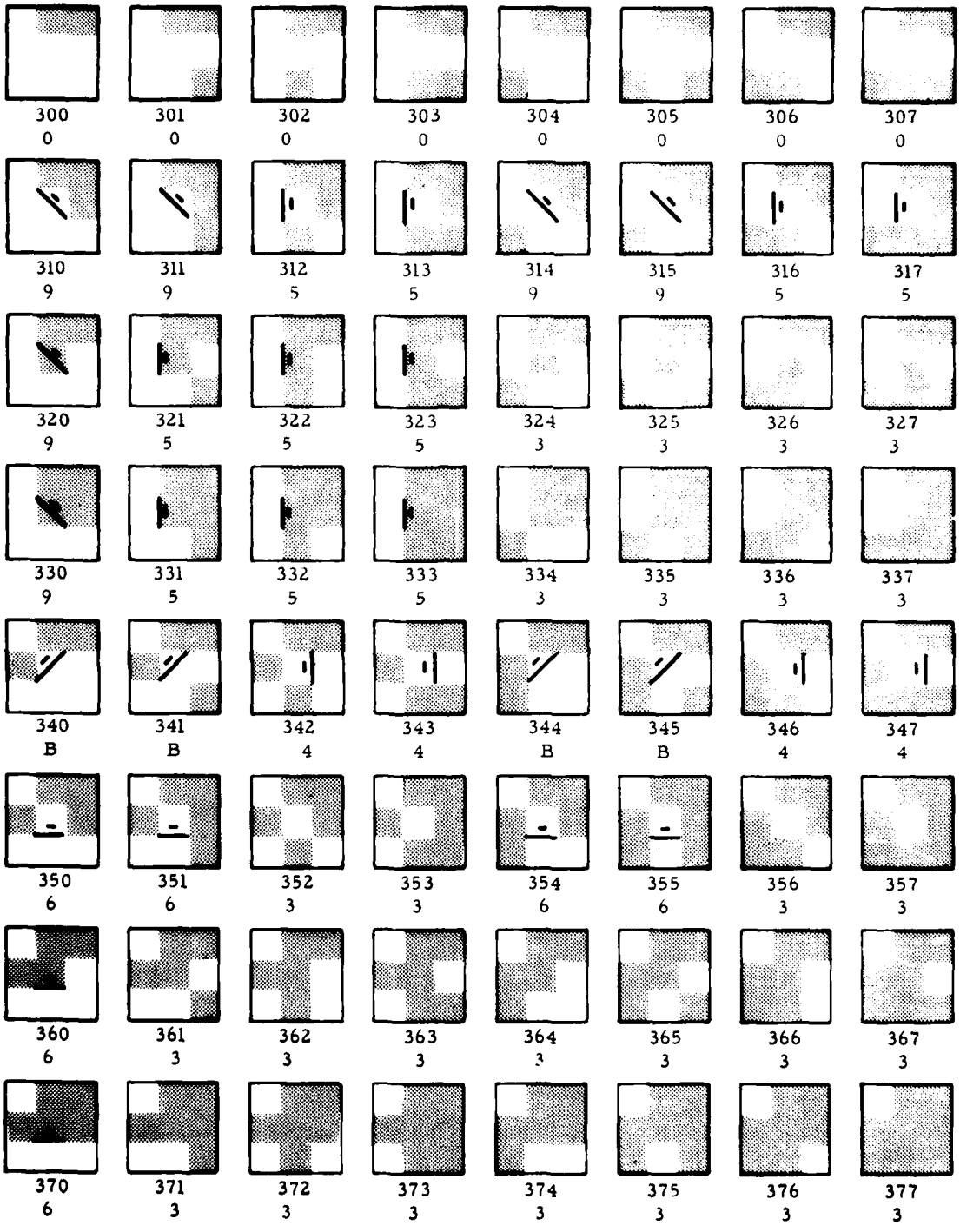
300 0
301 0
302 0
303 0
304 0
305 0
306 0
307 0
310 9
311 9
312 5
313 5
314 9
315 9
316 5
317 5
320 9
321 5
322 5
323 5
324 3
325 3
326 3
327 3
330 9
331 5
332 5
333 5
334 3
335 3
336 3
337 3
340 B
341 B
342 4
343 4
344 B
345 B
346 4
347 4
350 6
351 6
352 3
353 3
354 6
355 6
356 3
357 3
360 6
361 3
362 3
363 3
364 3
365 3
366 3
367 3
370 6
371 3
372 3
373 3
374 3
375 3
376 3
377 3

79-39-B-4

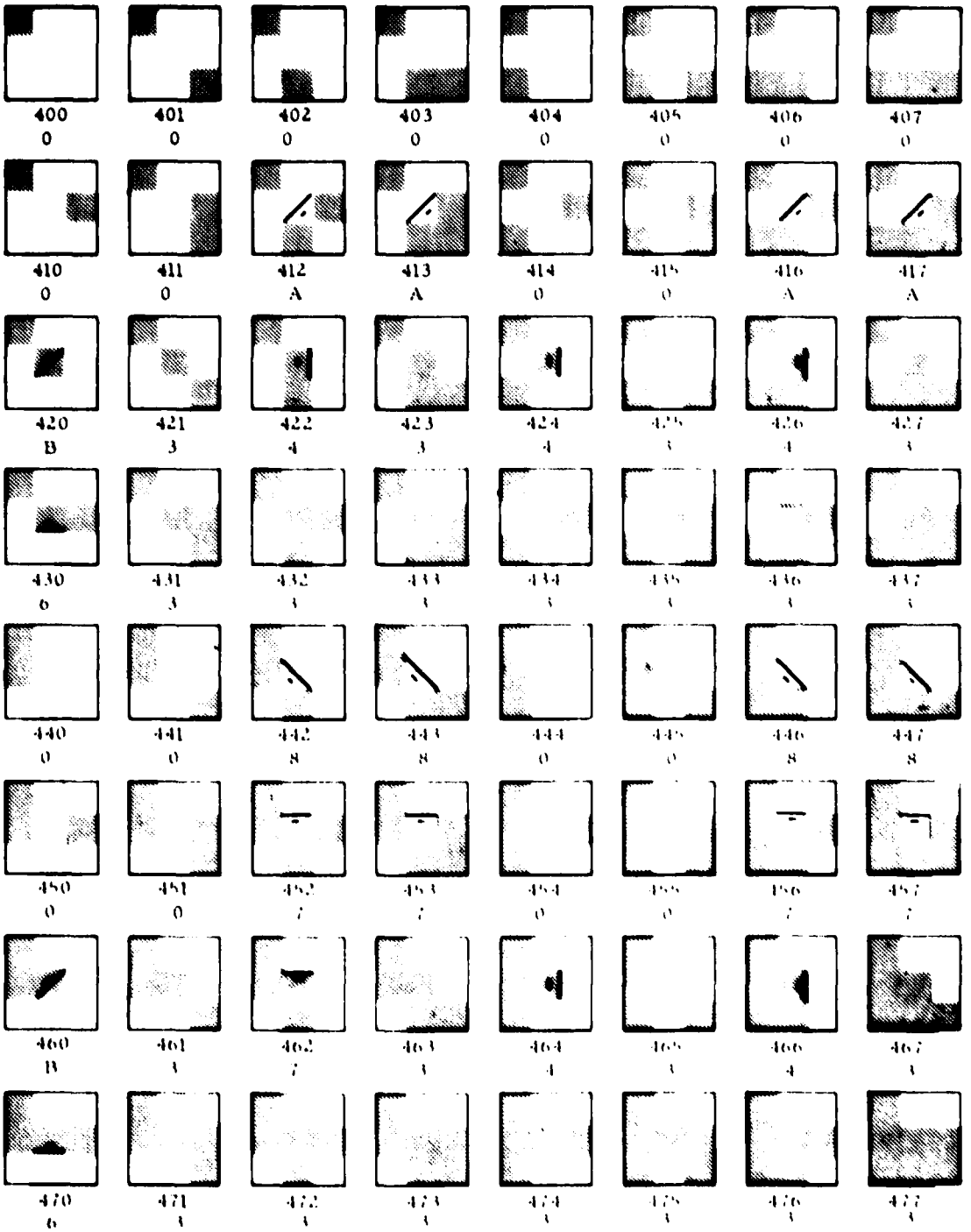
400 0
401 0
402 0
403 0
404 0
405 0
406 0
407 0
410 0
411 0
412 A
413 A
414 0
415 0
416 A
417 A
420 B
421 3
422 4
423 3
424 4
425 3
426 4
427 3
430 6
431 3
432 3
433 3
434 3
435 3
436 3
437 3
440 0
441 0
442 8
443 8
444 0
445 0
446 8
447 8
450 0
451 0
452 7
453 7
454 0
455 0
456 7
457 7
460 B
461 3
462 7
463 3
464 4
465 3
466 4
467 3
470 6
471 3
472 3
473 3
474 3
475 3
476 3
477 3

79-39-B-5

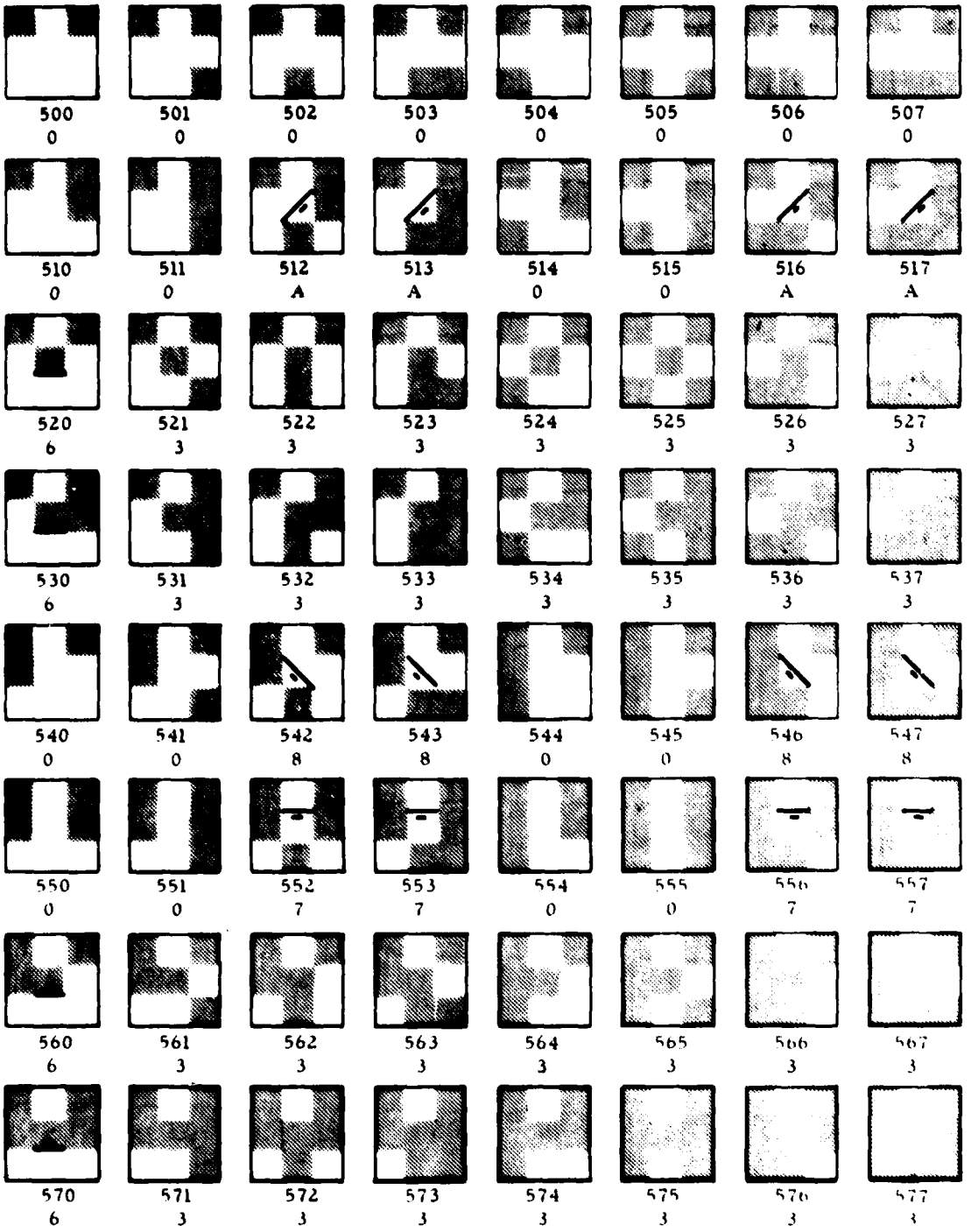
500 0
501 0
502 0
503 0
504 0
505 0
506 0
507 0
510 0
511 0
512 A
513 A
514 0
515 0
516 A
517 A
520 6
521 3
522 3
523 3
524 3
525 3
526 3
527 3
530 6
531 3
532 3
533 3
534 3
535 3
536 3
537 3
540 0
541 0
542 8
543 8
544 0
545 0
546 8
547 8
550 0
551 0
552 7
553 7
554 0
555 0
556 7
557 7
560 6
561 3
562 3
563 3
564 3
565 3
566 3
567 3
570 6
571 3
572 3
573 3
574 3
575 3
576 3
577 3

79-39-B-6

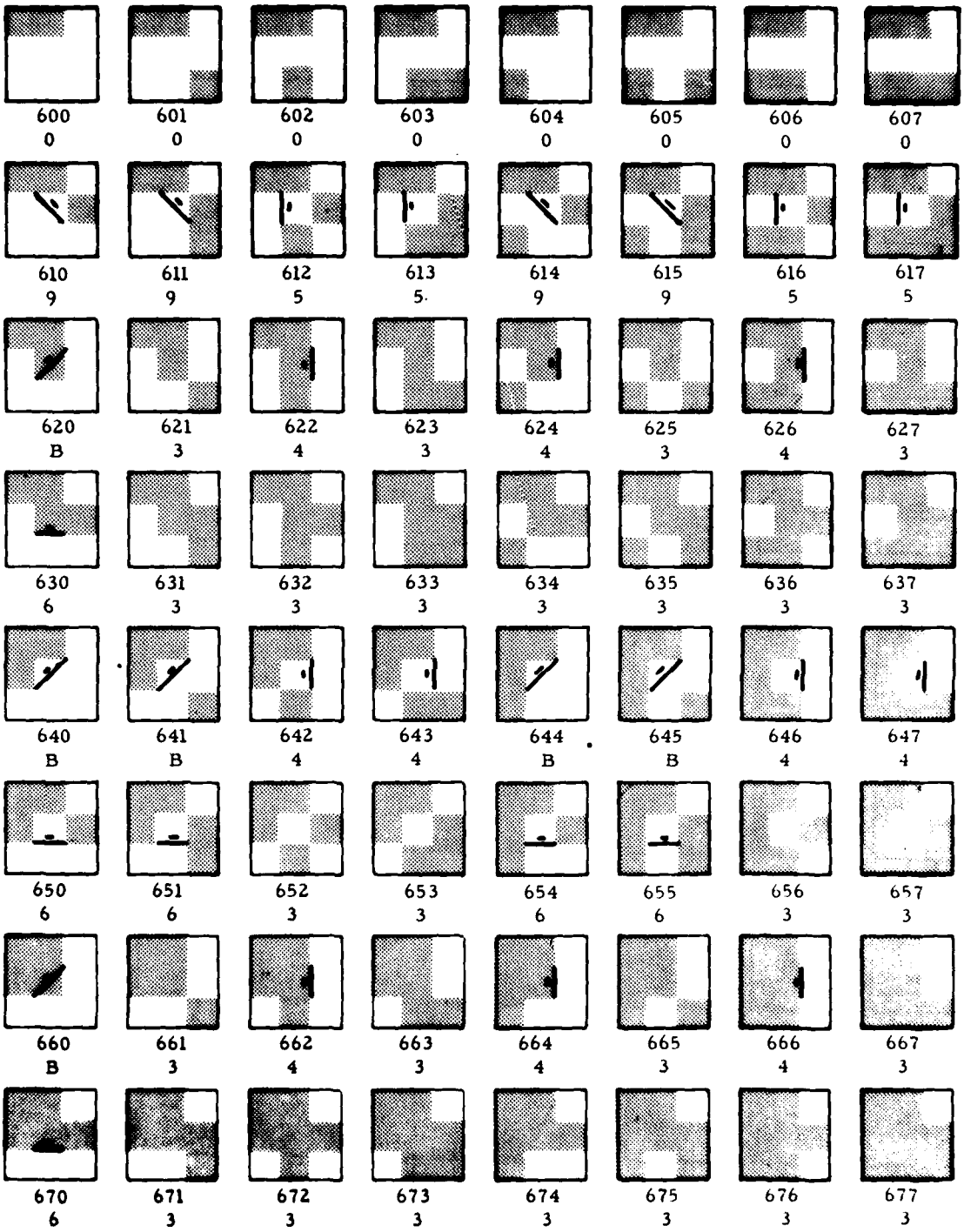
600
0
601
0
602
0
603
0
604
0
605
0
606
0
607
0
610
9
611
9
612
5
613
5
614
9
615
9
616
5
617
5
620
B
621
3
622
4
623
3
624
4
625
3
626
4
627
3
630
6
631
3
632
3
633
3
634
3
635
3
636
3
637
3
640
B
641
B
642
4
643
4
644
B
645
B
646
4
647
4
650
6
651
6
652
3
653
3
654
6
655
6
656
3
657
3
660
B
661
3
662
4
663
3
664
4
665
3
666
4
667
3
670
6
671
3
672
3
673
3
674
3
675
3
676
3
677
3

79-39-B-7

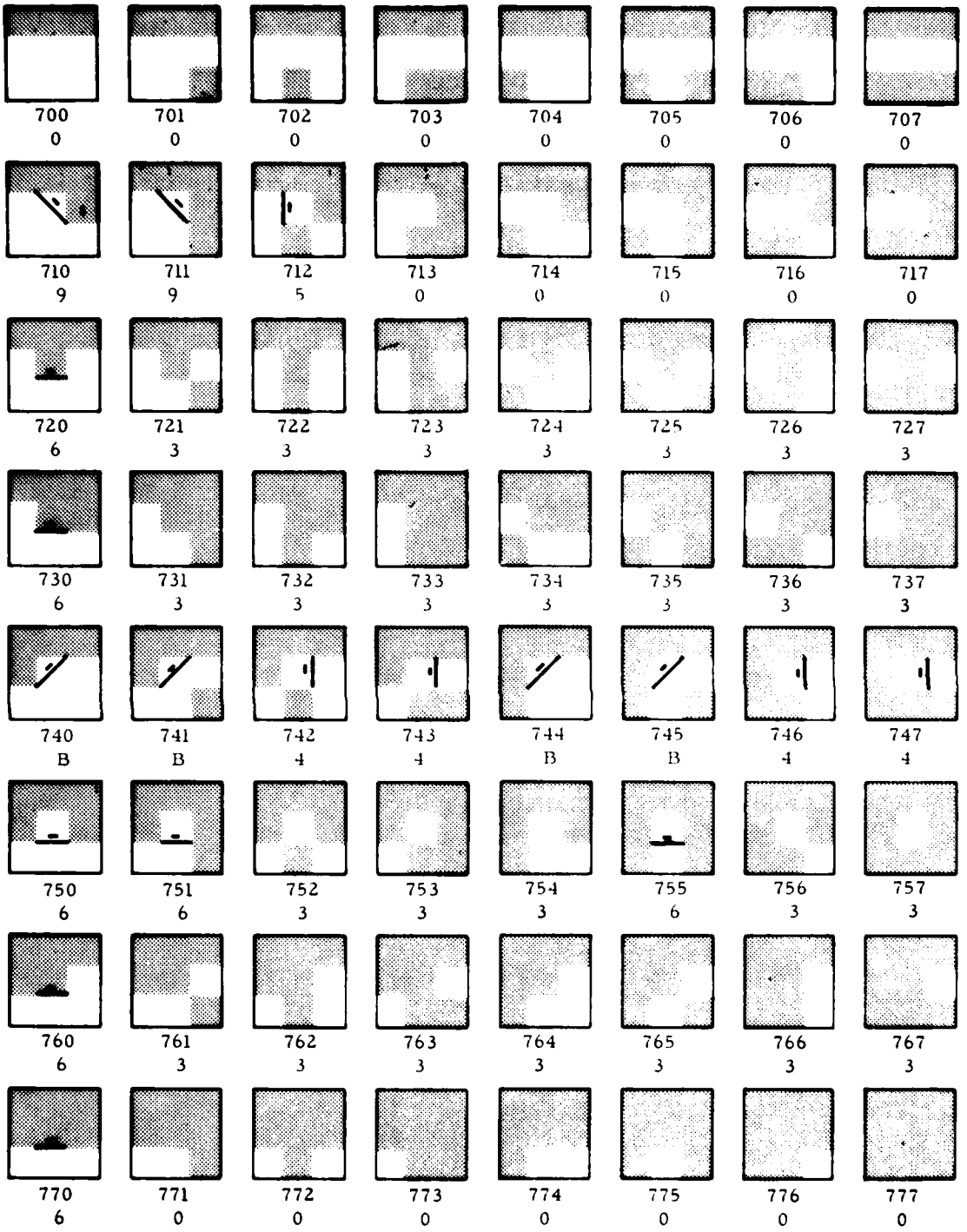
700 0
701 0
702 0
703 0
704 0
705 0
706 0
707 0
710 9
711 9
712 5
713 0
714 0
715 0
716 0
717 0
720 6
721 3
722 3
723 3
724 3
725 3
726 3
727 3
730 6
731 3
732 3
733 3
734 3
735 3
736 3
737 3
740 B
741 B
742 4
743 4
744 B
745 B
746 4
747 4
750 6
751 6
752 3
753 3
754 3
755 6
756 3
757 3
760 6
761 3
762 3
763 3
764 3
765 3
766 3
767 3
770 6
771 0
772 0
773 0
774 0
775 0
776 0
777 0

79-39-B-8

CHARACTER GENERATOR ROM

TYPE 00 LINES AND SPACES LINE

CHARACTER 0

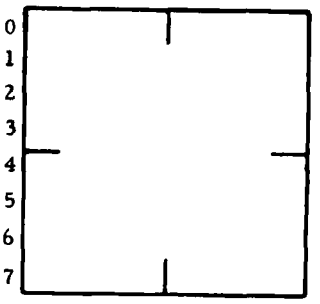

CHARACTER 1

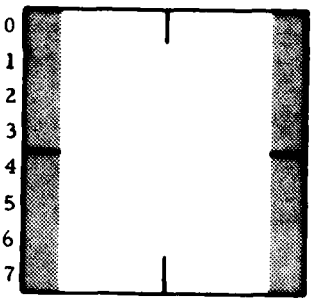

CHARACTER 2

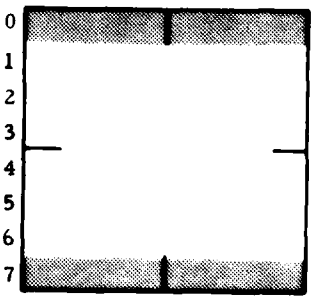

CHARACTER 3

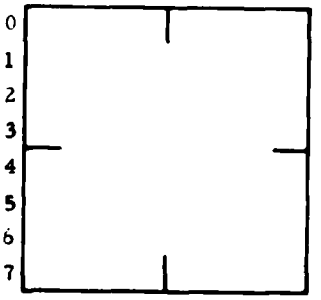

79-39-B-9

CHARACTER GENERATOR ROM

PARALLEL EDGES

TYPE 00 LINE

CHARACTER 4

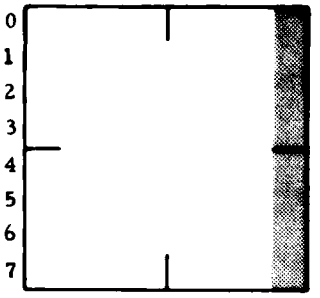

CHARACTER 5

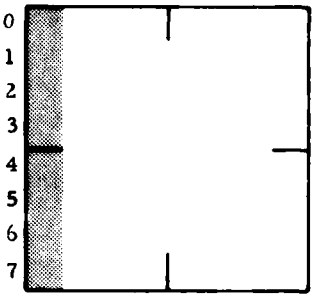

CHARACTER 6

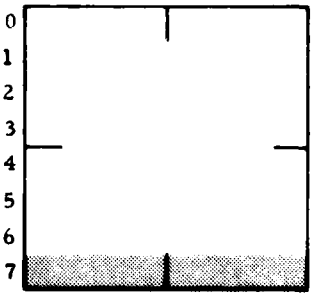

CHARACTER 7

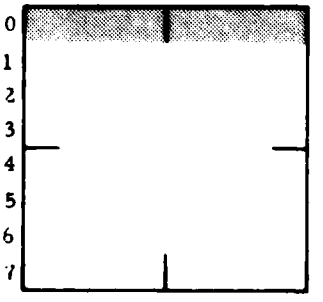

79-39-B-10

CHARACTER GENERATOR ROM

DIAGONAL EDGES

TYPE 00 LINE

CHARACTER 8

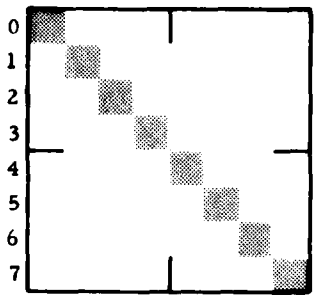

CHARACTER 9

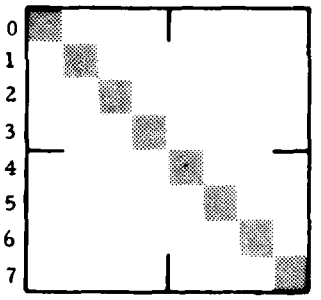

CHARACTER A

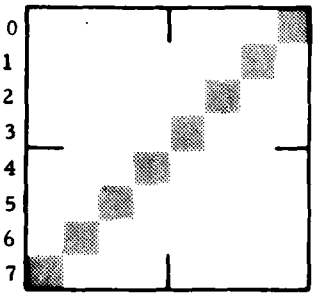

CHARACTER B

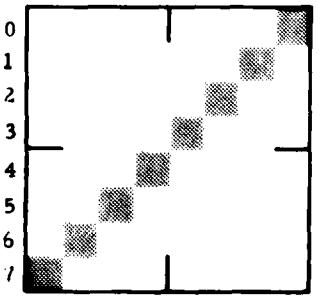

79-39-B-11

CHARACTER GENERATOR ROM

TYPE 00 ENDS LINE

CHARACTER C

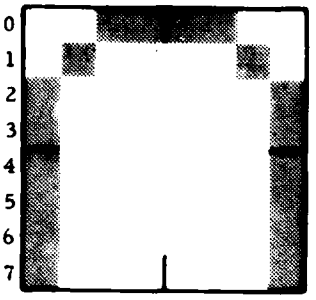

CHARACTER D

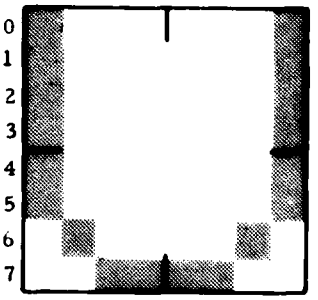

CHARACTER E

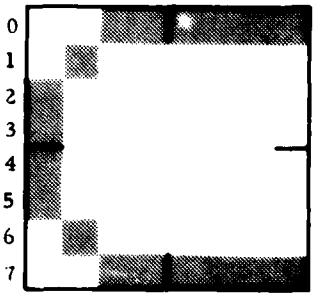

CHARACTER F

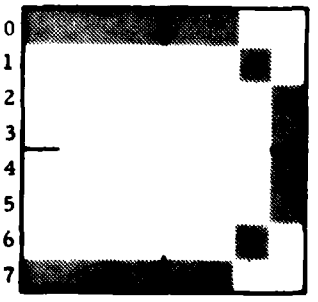

79-39-B-12

CHARACTER GENERATOR ROM

TYPE 01 LINES AND SPACES
LINE AND DOT

CHARACTER 0

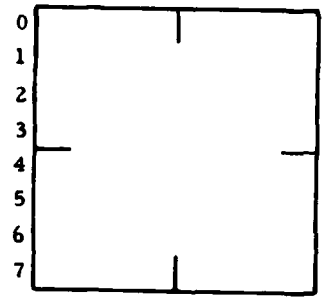

CHARACTER 1

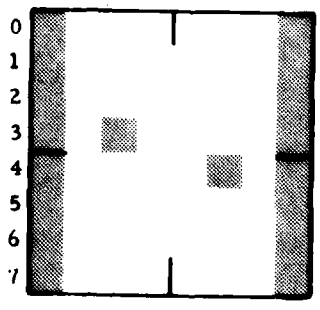

CHARACTER 2

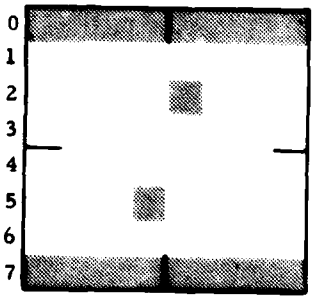

CHARACTER 3

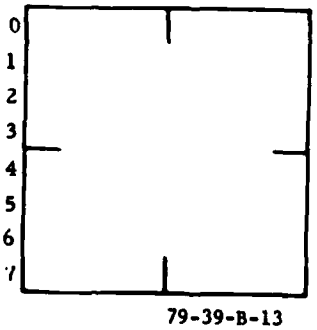

79-39-B-13

CHARACTER GENERATOR ROM

PARALLEL EDGES

TYPE 01 LINE AND DOT

CHARACTER 4

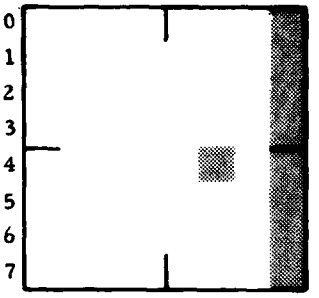

CHARACTER 5

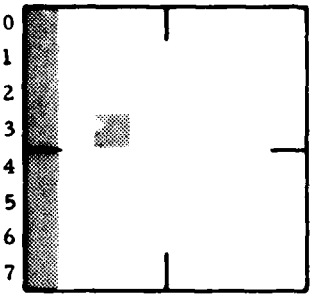

CHARACTER 6

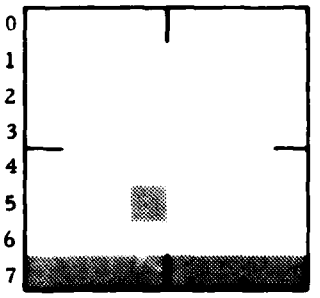

CHARACTER 7

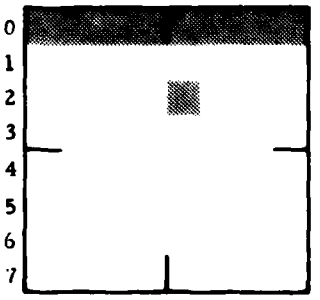

79-39-B-14

CHARACTER GENERATOR ROM

TYPE 01 DIAGONAL EDGES LINE AND DOT

CHARACTER 8

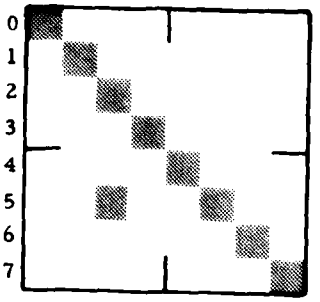

CHARACTER 9

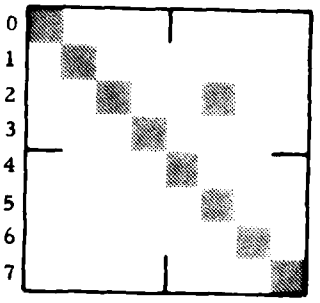

CHARACTER A

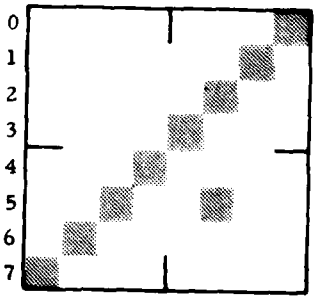

CHARACTER B

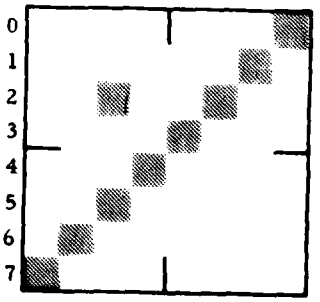

79-39-B-15

CHARACTER GENERATOR ROM

ENDS
TYPE 01 LINE AND DOT

CHARACTER C

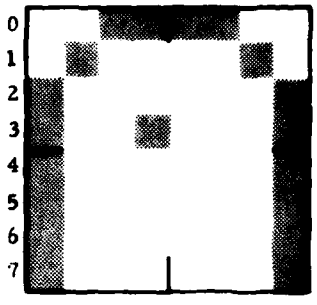

CHARACTER D

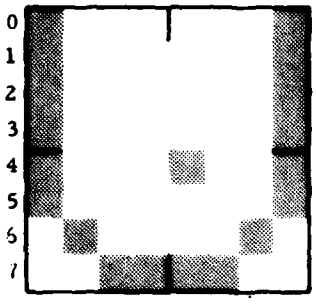

CHARACTER E

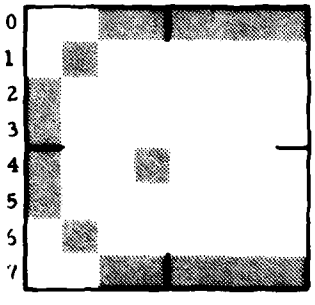

CHARACTER F

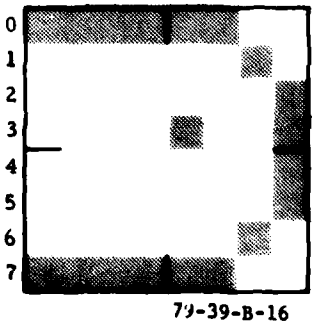

79-39-B-16

CHARACTER GENERATOR ROM

TYPE 10 LINES AND SPACES
10 SOLID

CHARACTER 0

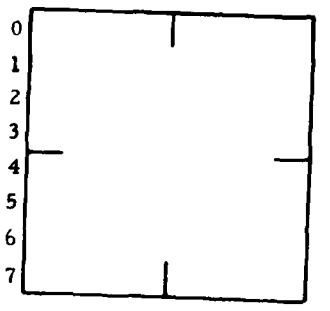

CHARACTER 1

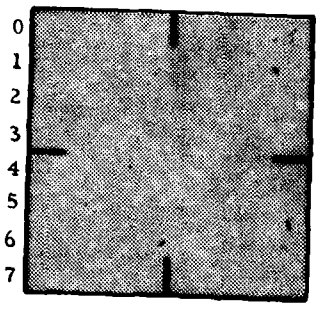

CHARACTER 2

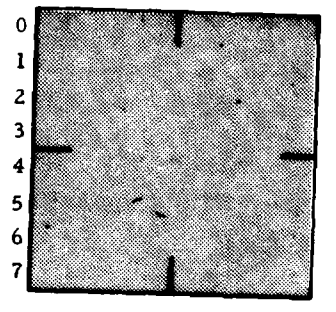

CHARACTER 3

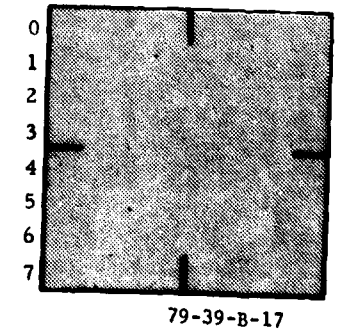

79-39-B-17

CHARACTER GENERATOR ROM

PARALLEL EDGES

TYPE 10 SOLID

CHARACTER 4

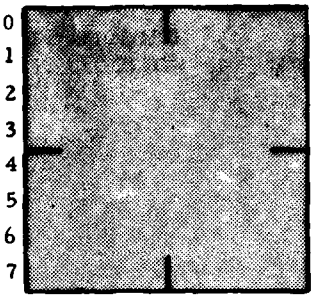

CHARACTER 5

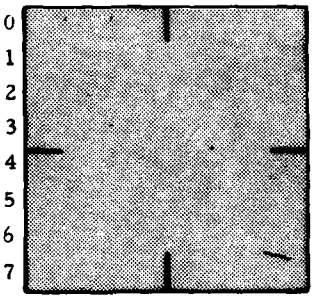

CHARACTER 6

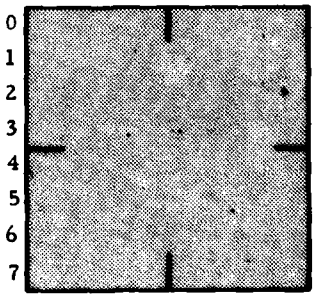

CHARACTER 7

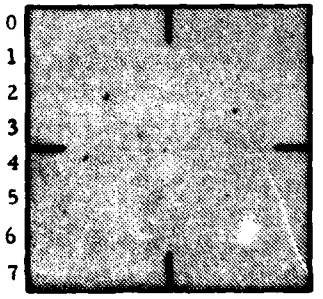

79-39-B-18

CHARACTER GENERATOR ROM

DIAGONAL EDGES

TYPE 10 SOLID

CHARACTER 8

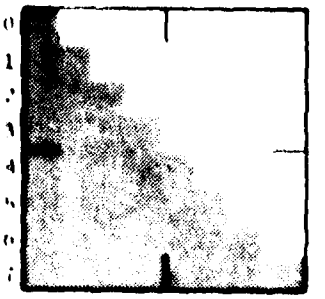

CHARACTER 9

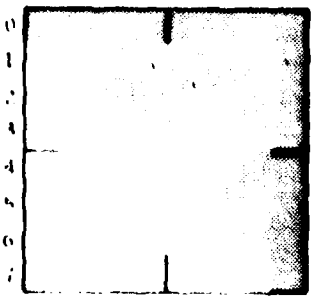

CHARACTER A

CHARACTER B

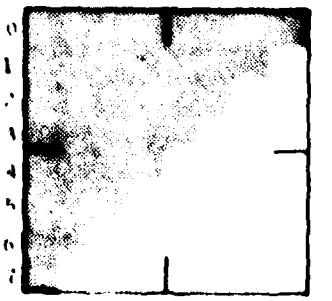

CHARACTER GENERATOR ROM

ENDS
TYPE 10 SOLID

CHARACTER C

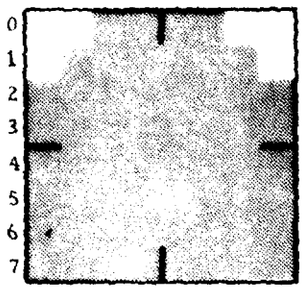

CHARACTER D

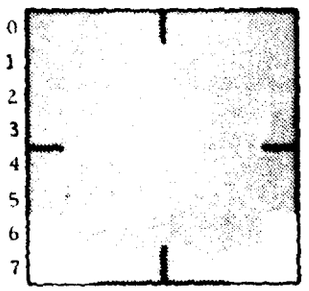

CHARACTER E

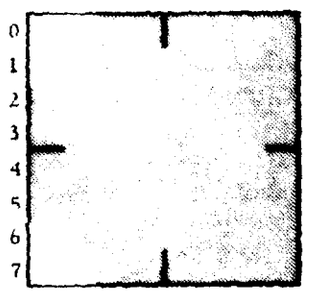

CHARACTER F

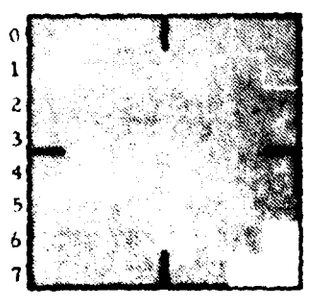

79-19-8-20

APPENDIX C

EFFECTIVE NUMBER OF SAMPLES AVERAGED BY A FIRST-ORDER DIGITAL FILTER

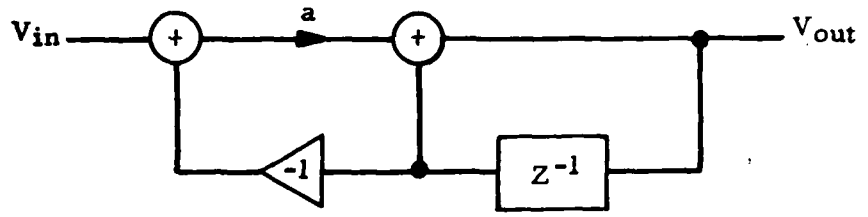

FIGURE C-1. BLOCK DIAGRAM

From the diagram (figure C-1)

$$V_{out} = z^{-1}V_{out} + a(V_{in} - V_{out}{}^{-1})$$

$$V_{out} = (1 - a)z^{-1}V_{out} + a\ Vin$$

$$V_{out} = (1-(1-a)z^{-1}) = a\ V_{in}$$

$$\frac{V_{out}}{V_{in}} = H(z) = \frac{a}{1-(1-a)z^{-1}}$$

by the inverse z transform $h(n) = a[1-a]^n$, where n is the sample number.

If $V = \Sigma a_n X$

$$\sigma_v^2 = \Sigma a_h^2 X_x^2$$

$$\sigma_{out}^2 = \Sigma h^2(n)\sigma_{in}^2 = \sigma_{in}^2 \Sigma h(n)^2$$

this results in a variance reduction of

$\frac{\sigma_{out}^2}{\sigma_{in}^2} = \Sigma h^2(n)$, which, for a uniform sampling is $\frac{\sigma_{out}^2}{\sigma_{in}^2} = \frac{1}{N}$.

Equating these two gives a measure of effective samples

$$\frac{1}{Ne} = \sum_{o}^{\infty} h^2(n) = \sum_{o}^{\infty} az[1-a]^{2n}$$

$$\frac{1}{Ne} = \frac{9^2}{1 - (1-a)^2}$$

$$\frac{1}{Ne} = \frac{a^2}{1-1+2a-a^2} = \frac{a}{2-a} = \frac{1}{\frac{2}{a}-1}$$

$$Ne = \frac{2}{a} - 1$$

for $a = \frac{1}{8}, \frac{1}{16}, \frac{1}{32}, \frac{1}{64}$

yields

Ne = 15, 31, 63, 127, respectively.